



HAL
open science

Rate dependent ductility and damage threshold: Application to Nickel-based single crystal CMSX-4

A. Mattiello, R. Desmorat, J. Cormier

► To cite this version:

A. Mattiello, R. Desmorat, J. Cormier. Rate dependent ductility and damage threshold: Application to Nickel-based single crystal CMSX-4. *International Journal of Plasticity*, 2019, 113, pp.74-98. 10.1016/j.ijplas.2018.09.006 . hal-02282589

HAL Id: hal-02282589

<https://hal.science/hal-02282589>

Submitted on 16 Apr 2024

HAL is a multi-disciplinary open access archive for the deposit and dissemination of scientific research documents, whether they are published or not. The documents may come from teaching and research institutions in France or abroad, or from public or private research centers.

L'archive ouverte pluridisciplinaire **HAL**, est destinée au dépôt et à la diffusion de documents scientifiques de niveau recherche, publiés ou non, émanant des établissements d'enseignement et de recherche français ou étrangers, des laboratoires publics ou privés.

Rate dependent ductility and damage threshold: application to Nickel-based single crystal CMSX-4

A. Mattiello^{a,b}, R. Desmorat^a, J. Cormier^c

^aLMT (ENS Cachan, CNRS, Université Paris Saclay), 94235 Cachan, France

^bSafran Helicopter Engines, Avenue Joseph Szydlowski, 64510 Bordes

^cInstitut Pprime, UPR CNRS 3346, Physics and Mechanics of Materials Departement, ISAE-ENSMA,
1 avenue Clément Ader, BP 40109, 86961 Futuroscope-Chasseneuil, France

Abstract

A phenomenological damage model is proposed to account for the strain rate dependency of the damaging processes at high temperature. Mechanical softening during tertiary creep and monotonic tension are modeled by an isotropic scalar internal variable D , whose evolution is described using a rate damage law $dD/dt = \dots$ governed by visco-plasticity and accounting for the enhancement by stress triaxiality. A novel rate sensitive damage threshold is introduced in order to reproduce the rate dependency of the onset of damaging processes. Damage evolution is coupled with the visco-plasticity model developed by the same authors for single crystal superalloys and accounting for microstructural evolution (like γ' -rafting and coarsening) in Desmorat et al (2017). The curves presented in this article are identified at 1050°C for the Ni base single crystal superalloy CMSX-4 but the proposed rate sensitive threshold modeling can be applied to other alloys showing a rate sensitive damage onset, as for example the single crystal superalloys MC2 but also the polycrystalline aggregate AD 730TM.

Key words: damage mechanics, Orowan stress, rafting, rate sensitive ductility, tertiary creep, visco-plasticity

1. Introduction

Nickel-based single crystal superalloys are state of the art materials for the design of high temperature components of aero-engines and land-based gas turbines for power generation (Pollock and Tin, 2006, Reed, 2006). They are typically used for the manufacturing of first stages of blades and vanes in such gas turbines and they can even be used for the manufacturing of intermediate and low pressure (uncooled) turbine blades in the most advanced engines for aircraft propulsion. During service operations, in addition to the degradation of the microstructure for temperature in excess of 900°C under the form of γ' rafting and/or coarsening (the interested reader is referred to previous publications describing the driving forces for γ' rafting (Kamaraj, 2003, Epishin et al, 2000, Reed et al, 1999)), different kind of damage may develop along a blade profile, involving creep and/or fatigue and/or oxidation assisted damage, depending on the type of engine and operating conditions. As an example, creep is the main life limiting solicitation for uncooled turbine blades while thermo-mechanical fatigue damage are mainly observed for internally cooled components (Zhang, 2016). In the present paper, a special focus will be paid to damage, with a special emphasis on identifying when its development, in the sense of a loss of the load bearing capacity, has a major contribution to creep acceleration and monotonic tension softening. Given the variety in creep curves shapes that can be encountered when changing creep conditions (Svoboda and Lukas, 1998, Reed et al, 1999, Matan et al, 1999a, Reed, 2006, Kindrachuk and Fedelich, 2012), it is often difficult to clearly identify when cavitation or development of cracks are really active based on the macroscopic creep curve. Damage, in the sense of a loss of load bearing section, may already be active at low temperature/high stress despite no clear tertiary creep stage is noticed (MacLachlan et al, 2002, MacLachlan and Knowles, 2001, MacLachlan et al, 2001), while at high temperature, a continuous creep acceleration may be noticed (Epishin et al, 2001, Matan et al, 1999b), without any noticeable increase in porosity, both in terms of pores density and pore volume fraction. Indeed, as noticed recently by le Graverend et al (2017) using MC2 first generation Ni-based single crystal superalloy followed by X-ray tomography, the onset of tertiary creep in the 900°C-1100°C temperature range results from the γ/γ' microstructure degradation, under the form of a topological inversion (Epishin et al, 2001, Matan et al, 1999b, Caron et al, 2008, Epishin et al, 2000). This kind of microstructure degradation may be qualified as a microstructural damage and is sometimes considered as a “true” damage (McLean and Dyson, 2000), even if not inducing a loss of stiffness or load bearing capacity. Reed et al (2007) also observed that the very steep tertiary creep at 1150°C / 100 MPa in CMSX-4 Ni-based single crystal superalloy is not controlled by the initial pore volume/size. Indeed, creep lifetimes of this alloy under these creep conditions remain unaffected after applying a Hot Isostatic Pressing (HIP) treatment devoted to close pores. A similar conclusion was observed more recently by Steuer et al (2015) comparing creep properties in a wide temperature range (from 750°C to 1200°C) using AM1 Ni-based single crystal superalloys

Email address: adriana.mattiello@safrangroup.com (A. Mattiello)

processed using either a Liquid Metal Cooling or a standard Bridgman solidification techniques (both techniques leads to different pore size distribution). Similar questions also arise about the monotonic tensile response. Many literature studies show that at high temperatures ($T > 900^\circ\text{C}$) and low strain rates ($\approx 10^{-5}\text{s}^{-1}$) the monotonic tensile response of this class of materials is characterized by the same deformation/damage mechanisms observed during creep (Gabrisch et al, 1994, Cormier, 2006, Diologent, 2002, Giraud, 2013). Hence, damage mechanisms (i.e. cavitation and γ' shearing) contribute to the degradation of the mechanical properties only when a certain amount of softening —and thus of plastic deformation— has already been produced. Different deformation/damaging mechanisms are instead observed during monotonic tensile tests performed at high temperature and higher strain rates. In this case no time is left to the microstructure to evolve and to cavities to diffuse. Thus, deformation is produced by the progressive filling of constant-size matrix channels by dislocations. Plastic damage, enhanced by necking, takes places only at the end of the tests. Overall creep and tensile test results thus suggest that the mechanical damage onset is a rate governed phenomenon.

In the context of Continuum Damage Mechanics (Lemaitre and Chaboche, 1985,1991, Lemaitre, 1992), kinetic damage laws with loading dependent damage thresholds have been introduced: in the works of Lemaitre (1984) for ductile rupture and Lemaitre and Doghri (1994) for High Cycle Fatigue and of Sermage et al (2000), Desmorat and Otin (2008), Marull (2011), Chaboche et al (2013), Marull and Desmorat (2013) for creep-fatigue. In these works, the loading dependency of the accumulated plastic strain at damage initiation is due to a formulation of the damage threshold in terms of stored energy density (Lemaitre and Desmorat, 2005). The corresponding constitutive equations apply to creep and fatigue —of a $2\frac{1}{4}$ Cr Mo steel, of HA188 alloy and of AM1 and CMSX-2 single crystal superalloys— but they do not model the ductility in monotonic tension, the ductility being defined as the strain to fracture. A damage threshold has recently been considered in the works of Cornet et al (2011), of Krairi and Doghri (2014) and, for MC2 single crystal superalloy, of le Graverend et al (2014a). It has been made multiaxiality dependent in (Murakami and Hayakawa, 1998, Bouchard et al, 2011, Cao et al, 2014).

To answer the key question, which is when so-called mechanical damage starts to have a prominent contribution to the material mechanical response, one will next use a microstructure modeling approach recently developed for single crystal superalloys (Desmorat et al, 2017) and identified at 1050°C for the CMSX-4 alloy. This visco-plastic model (whose key points are described in the section 7), accounts for the γ' -rafting, coarsening and dissolution. According with what observed by le Graverend et al (2017), it is intended to describe the degradation of the mechanical response until the first stage of tertiary creep (up to $\approx 2 - 5\%$ of plastic deformation) and the first mechanical softening observed during slow monotonic tension (up to $\approx 10\%$ of plastic deformation). The objective of the continuum damage modeling proposed in this article is then to describe the last stage of creep as well as monotonic the tensile response of single crystal superalloys. The curves presented next are identified on the tests considered in Desmorat et al (2017), but specific experimental tests have been performed expressly for the present study in order to enrich the experimental database for the mechanical modeling.

Moreover, the formulation of Kelvin projectors for cubic materials will be based on the harmonic decomposition of the elasticity tensor \mathbb{E} having cubic material symmetry (Backus, 1970, Onat, 1984, Olive et al, 2017b). This will allow us to compute Kelvin projectors without using the spectral decomposition.

Finally, it has to be highlighted that a rate sensitive ductility at high temperature has been observed not only for single crystal superalloys (Gabrisch et al, 1994, Cormier, 2006), but also for other materials presenting very different deformation/damage mechanisms. Examples are the nano-twinned crystal of pure copper (Lu et al, 2005), the oxide dispersion strengthened (ODS) steels (Steckmeyer, 2012) and the polycrystalline aggregates AD 730TM (Thébaud et al, 2016), which all show a positive rate sensitivity of the (mechanical) damage onset and, as a consequence, a positive rate sensitivity of the ductility. Thus, the damage model proposed in this article can be used for modeling the monotonic mechanical response of other materials, having visco-plastic properties different from the one observed for single crystal superalloys. Further details are given in next section, where the damage modeling issues for CMSX-4 and AD 730TM are described.

2. Background and motivations

As mentioned, a positive rate sensitive ductility has been observed on γ' hardened superalloys such as the AD 730TM and the CMSX-4 (Fig. 1 and Fig. 3).

For the AD 730TM this rate dependency can be attributed to oxidation: higher loading rates lead to a shorter interaction with the environment and to a lower time to rupture (Fig. 1, Thébaud et al (2016)),

- at high strain rate $\dot{\epsilon}$, the specimens deform until the plastic damage —enhanced by necking— classically leads to rupture (Kachanov, 1958, Rabotnov, 1969): in this case oxidation does not play a main role in the damage process,
- inversely, during the tests performed at lower strain rate ($\dot{\epsilon} = 10^{-4}\text{s}^{-1}$ in Fig. 1), oxidation has enough time to develop and to contribute to the degradation of the material.

Fig. 2 is a post-mortem observation of an AD 730TM Fine Grain (FG) specimen tested under tensile creep at 700°C and 250 MPa. Since AD 730TM FG is a polycrystal, oxidation takes place at grain boundaries and it is present even at 700°C .

CMSX-4 has no grain boundaries, it is a Ni based single crystal superalloy. Its oxidation is observed only at temperature in excess of 900°C and this phenomenon does not impact significantly the mechanical response of the material (Reed, 2006). At such temperature levels, the main causes of the material degradation are

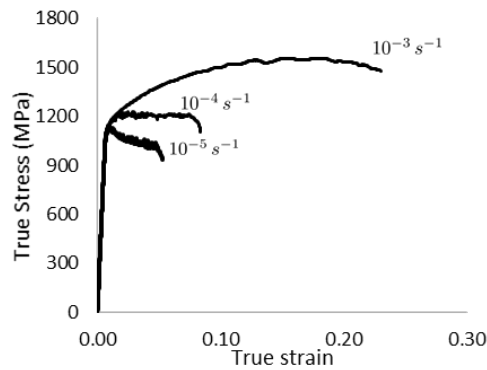


Figure 1: AD 730™ Fine Grain (FG): uniaxial tension tests at 750°C (Thébaud et al, 2016)

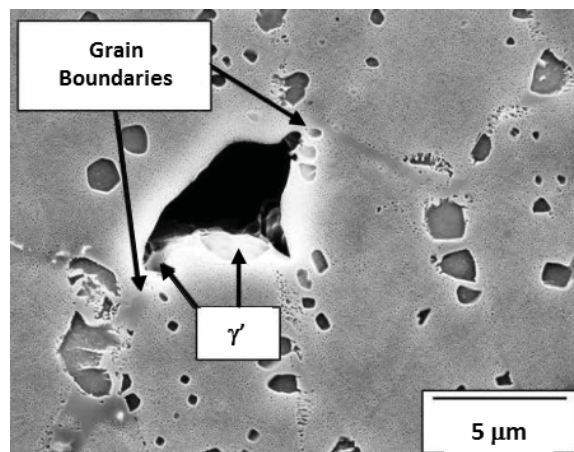


Figure 2: AD 730™ Fine Grain (FG): post-mortem observation after tensile creep 700°C and 250 MPa (Thébaud et al, 2016).

- first, the microstructural evolution of the γ' phase, *i.e.* the rafting phenomenon (Tien and Copley, 1971, Tien and Gamble, 1972, Caron and Khan, 1983, Draper et al, 1989, Pollock and Argon, 1994, Reed et al, 1999)),
- second, *after a non negligible threshold*, the standard plastic damage (le Graverend et al, 2017, Link et al., 2006, Srivastava and Needleman, 2015).

Two types of microstructural evolution affect the CMSX-4 response: the rafting and coarsening of the hardening phase.

The first consist in a morphology change of the cubic $\gamma - \gamma'$ microstructure. The coexistence of the two γ/γ' crystal phases having different lattice parameters produces internal residual stresses at the microscale (Pollock and Argon, 1994, Kamaraj, 2003). When the equilibrium of the internal stress is perturbed by the external loads, the potentials of the chemical species change and a diffusive phenomenon, enhanced by visco-plasticity, takes place (Biermann et al., 1996, Epishin et al, 2000, Mughrabi, 2009). The mass transport direction depends on the crystal direction solicited and cause the migration of the hardening species from the more loaded to the less loaded matrix channels. During tensile creep along $\langle 001 \rangle$ this leads to the saturation of vertical channels and to the widening of the horizontal ones (Fig. 4). Precipitates then became plate-shaped and γ horizontal channel appear wider and longer. Since the direction of such a diffusive phenomenon depends on the internal stress state, the γ' coalescence depends on the crystallographic orientation and it tends to respects the crystal symmetry. A different morphology of the degraded microstructure is observed if the loading is performed along $\langle 111 \rangle$ crystallographic orientation, called "mechanical coarsening" of the γ' phase as the γ channel widths equally increase in the three space directions (Fig. 5). The γ' coarsening consist of an Ostwald-ripening like phenomenon (Ostwald, 1897). This consists in a homothetic growth of the $\gamma - \gamma'$ (cubic or plate-shaped) microstructure which causes an additional widening of the active γ channels.

Concerning the observation technique, mirror surface finish has been realized after slow cooling by performing mechanical polishing up to 4000 SiC with grit papers and then by polishing with $3\mu\text{m}$ and $1\mu\text{m}$ diamond solutions. A final chemical etching with aqua regia ($1/3 \text{HNO}_3 + 2/ \text{HCl} / \text{vol. part}$) has been used to reveal the γ/γ' microstructure. Scanning Electron Microscopy (SEM) is realized using a Jeol 7000F microscope.

These microstructural evolutions have a detrimental impact, *time dependent*, on the tensile response (Gabrisch et al, 1994, Diologent, 2002): as in the oxidation case, the diffusive process has time to set when the loading rate is low enough. For this reason a gradual softening is observed during the tensile test at 10^{-5}s^{-1} on a $\langle 001 \rangle$

oriented CMSX-4 specimen (Fig. 3a, the linear part of the softening up to $\varepsilon \approx 0.15$ is at zero damage). On the contrary, a higher loading rate leads to shorter time to rupture but larger rupture strain: the tensile tests at strain rates $\dot{\varepsilon} \geq 10^{-4} \text{s}^{-1}$ are too quick for the γ' evolution to occur.

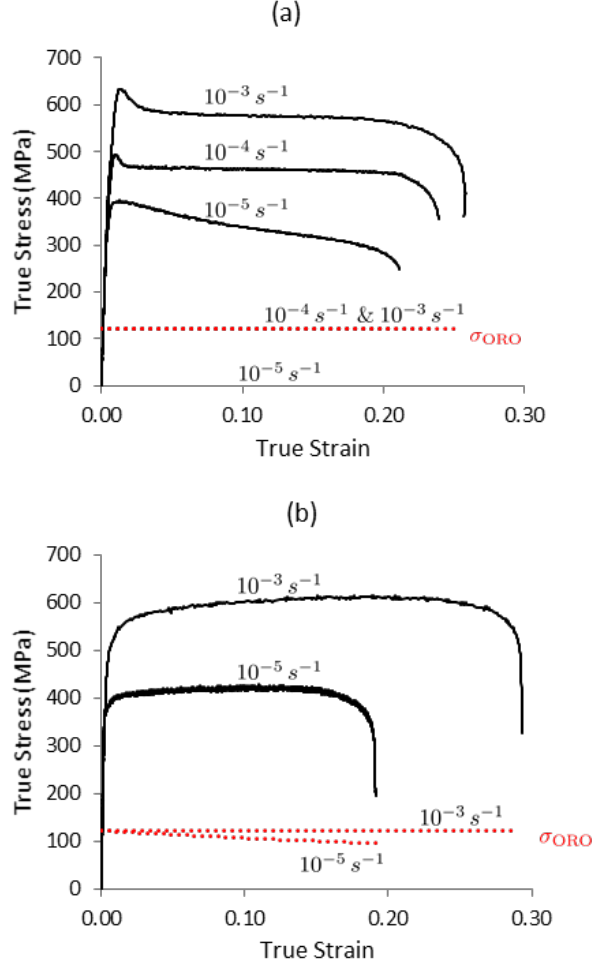


Figure 3: Stress-strain curves of CMSX-4 at different strain rates (1050°C). Computed Orowan stress σ_{ORO} reported. (a) crystallographic orientation $\langle 001 \rangle$, (b) crystallographic orientation $\langle 111 \rangle$.

The main cause of the initial plastic strain (convex) acceleration in creep of CMSX-4 at 1050°C is the microstructure degradation (Fig. 4). It is not mechanical damage: indeed it has been shown that microcracks or cavities growth takes place in a second step (le Graverend et al, 2017). As observed in Fig. 6, final failure at different applied stresses results from the linkage of micro-cracks initiated from different interdendritic casting pores. Indeed, these pores, already present before any inelastic deformation, may coarsen during high temperature/low stress creep (see, e.g., Link et al. (2006)). According to Fig. 6, it is seen a greater density of cracked casting pores close to the fracture surface due to a locally higher triaxiality. According to le Graverend et al (2017), such a kind of pore cracking —represented next by scalar damage variable D — occurs in the very last stages of the creep curve, far in excess of 1-2 percent(s) creep strain under the investigated creep conditions.

Thus, continuous damage D in the sense of Continuum Damage Mechanics occurs only when a sufficient amount of plastic deformation, p_D , is reached. Such a damage threshold is also observed in monotonic tension (the onset of final acceleration of the softening in Fig. 3): concerning the tests at $\dot{\varepsilon} \geq 10^{-4} \text{s}^{-1}$, for which almost no microstructural evolutions take place, the samples deform first with a plateau (no damage); the plastic damage, enhanced by necking, occurs only in a second stage at large enough plastic strains (> 0.18).

From a mechanical point of view, previous observations allow us to define a damage threshold p_D in terms of accumulated plastic strain $p = \int (\frac{2}{3} \dot{\varepsilon}^p : \dot{\varepsilon}^p)^{1/2} dt$, such as as long as the accumulated plastic strain remains below p_D there is no damage growth (Lemaitre, 1984):

$$p < p_D \quad \longrightarrow \quad D = 0 \quad (1)$$

Contrary to standard results (Lemaitre, 1992, Lemaitre and Doghri, 1994, Sermage et al, 2000), the damage threshold will next be made dependent, in an original manner, on the accumulated plastic strain rate. Remark that threshold p_D

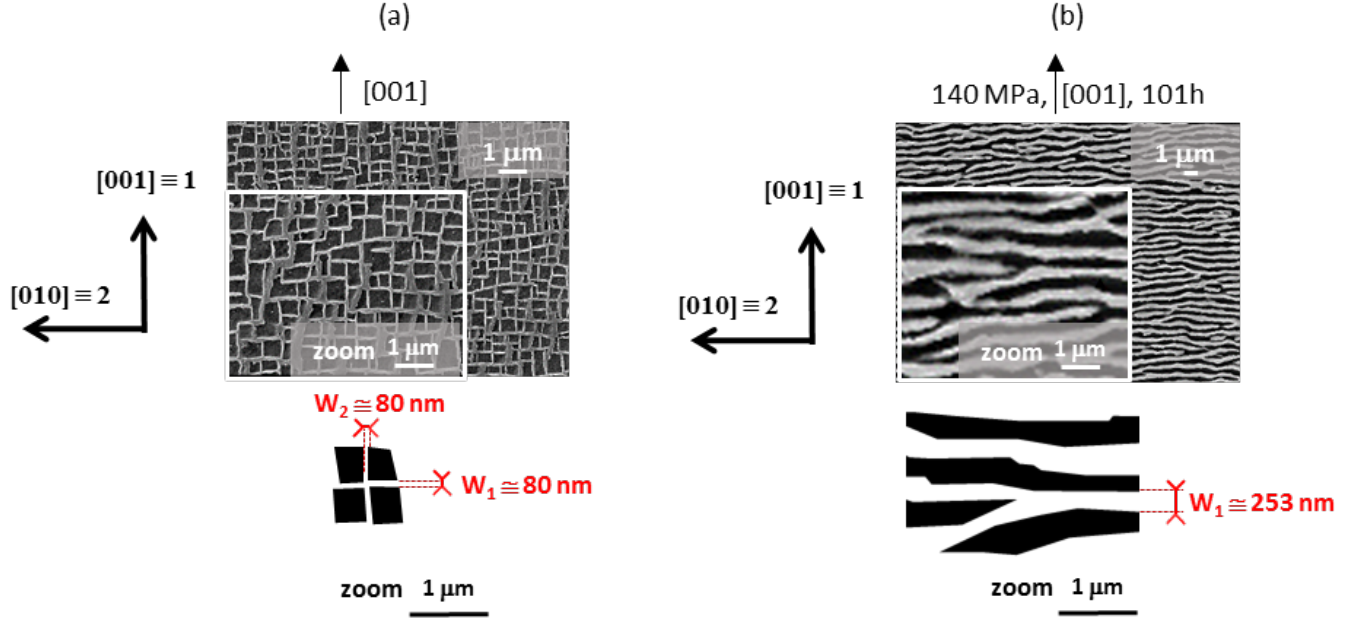


Figure 4: γ/γ' microstructure evolution (rafting) of CMSX-4 Ni-based single crystalline superalloys: (a) initial morphology at 1050°C, γ channel widths $w_1 \approx w_2 \approx w_3 \approx w_0$, (b) after 101 h of creep at 1050°C and 140 MPa along $\langle 001 \rangle$, $w_1 > w_0$ and $w_2 = w_3 = 0$.

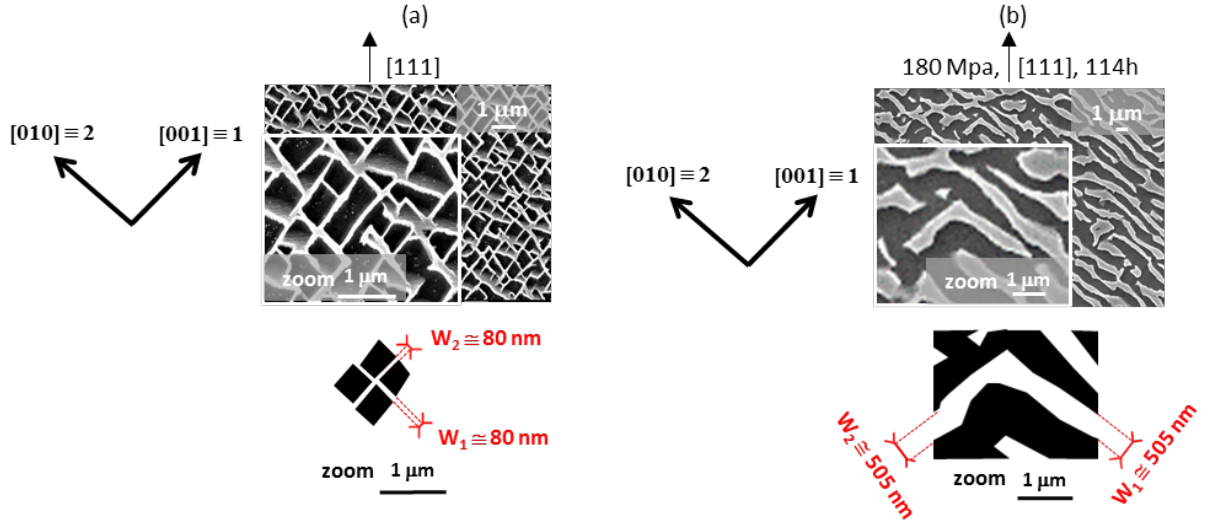


Figure 5: γ/γ' microstructure evolution of CMSX-4 Ni-based single crystalline superalloys: (a) initial morphology at 1050°C, γ channel widths $w_1 \approx w_2 \approx w_3 \approx w_0$, (b) morphology after 67 h of creep at 1050°C and 200 MPa along $\langle 111 \rangle$, $w_1 \approx w_2 \approx w_3 > w_0$.

- is of the order of magnitude of a few percent in creep (assumed to be the limiting case $\dot{p} \approx 0$),
- and reaches almost 0.2 (*i.e.* 20%) in tension at 10^{-3}s^{-1} .

Proposed modeling will be applied to CMSX-4 superalloy. In order to account for the rafting phenomenon and for the mechanical damage, both in creep and in tension at different strain rates, we use then the tensorial representation of the γ channel width proposed in (Desmorat et al, 2017). Kelvin modes based formulations of anisotropic (cubic) visco-plasticity (Cowin et al, 1991, Biegler and Mehrabadi, 1995, François, 1995, Bertram and Olschewski, 1996, Arramon et al., 2000, Mahnken, 2002, Desmorat and Marull, 2011) will be introduced and a link between Kelvin decomposition and harmonic decomposition of cubic elasticity made (Section 4).

The decrease of the yield stress and the acceleration of plastic strain rate due to γ' rafting phenomenon are attributed to Orowan stress, inversely proportional to the γ channel width (Benyoucef et al., 1993, Fedelich et al, 2009, Tinga et al, 2009, Cormier and Cailletaud, 2010a, Staroselsky et al, 2011), denoted σ_{ORO} when directly summed to yield stress σ_y in a macroscopic criterion function, possibly anisotropic. Fig. 3 shows that it evolves only at low strain rate $\dot{\epsilon} \leq 10^{-5}\text{s}^{-1}$ (dotted lines, CMSX-4 at 1050°C).

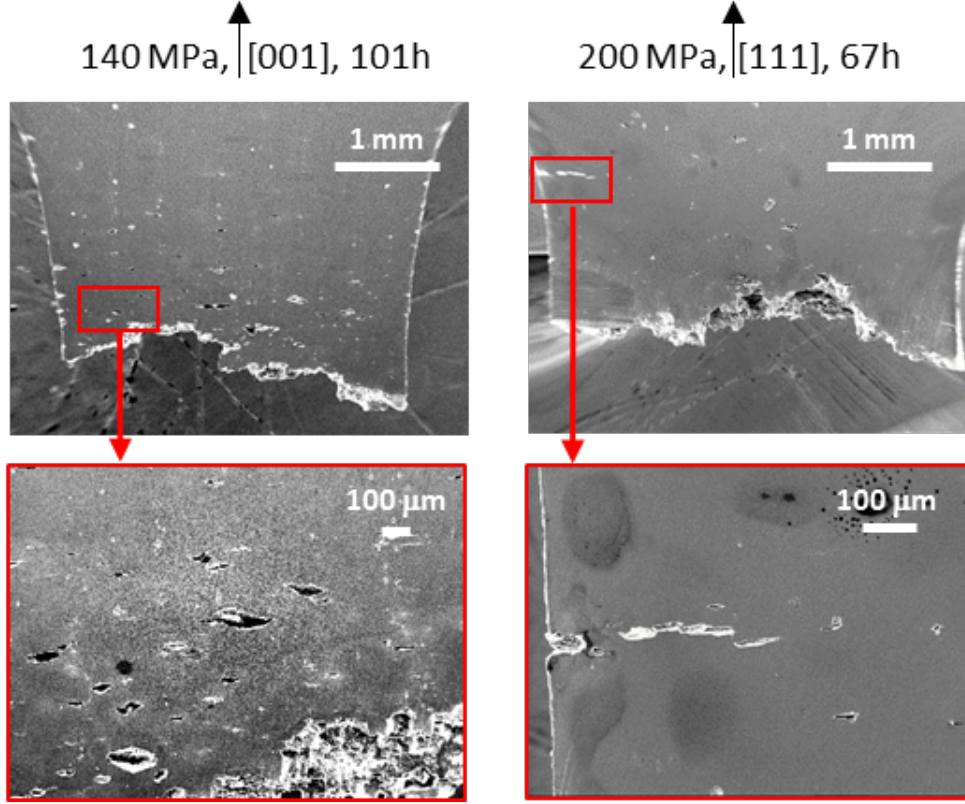


Figure 6: Post-mortem observations of CMSX-4 specimens, after a creep test at 1050°C and 140 MPa (left), and after a creep test at 1050°C and 200 MPa (right).

3. Generalities on continuous damage

Isotropic damage evolution laws for metals are mainly of two kinds: micromechanically based and phenomenological. To the first kind belong the Rice-Tracey-Gurson porosity growth damage models (Rice and Tracey, 1969, Gurson, 1977, Tvergaard and Needleman, 1984), extended to visco-plasticity in (Pan et al, 1983, Tvergaard and Needleman, 1986, Leblond et al, 1994, Hao and Brocks, 1997, Gaffard et al, 2005, Besson, 2009a, Mbiakop et al, 2015, Srivastava and Needleman, 2015, Ling et al, 2017). To the second kind belong the pioneering damage models for tertiary creep (Kachanov, 1958, Rabotnov, 1969) and the Lemaitre-Chaboche phenomenological damage models (Lemaitre and Chaboche, 1985, 1991, Lemaitre and Dufailly, 1987, Lemaitre, 1992, Altenbach and Kruch, 2013), coupled to visco-plasticity in (Chaboche, 1979, Benallal et al, 1988, Saanouni and Chaboche, 1989, Saanouni et al, 1994, Sermage et al, 2000, Lemaitre and Desmorat, 2005, Krairi and Doghri, 2014). For both families of models, including for first kind the representation of void nucleation (Chu and Needleman, 1980), the damage rate is proportional to the accumulated plastic strain rate \dot{p} and enhanced by the stress triaxiality

$$T_X = \frac{\sigma_H}{\sigma_{eq}} = \frac{1}{3} \frac{\text{tr} \boldsymbol{\sigma}}{\sigma_{eq}} \quad (2)$$

with $\sigma_H = \frac{1}{3} \text{tr} \boldsymbol{\sigma}$ the hydrostatic stress and $\sigma_{eq} = (\frac{3}{2} \boldsymbol{\sigma}' : \boldsymbol{\sigma}')^{1/2}$ von Mises (1928) stress, $(\cdot)' = (\cdot) - \frac{1}{3} \text{tr}(\cdot) \mathbf{1}$ denoting the deviatoric part.

The stress level has a strong effect in Lemaitre's damage law when written, for $p \geq p_D$ (Lemaitre and Dufailly, 1987)

$$\dot{D} = \left(\frac{Y}{S}\right)^s \dot{p} \quad Y = \frac{1}{2} \boldsymbol{\epsilon}^e : \mathbf{E} : \boldsymbol{\epsilon}^e = \frac{1}{2} \tilde{\boldsymbol{\sigma}} : \mathbf{E}^{-1} : \tilde{\boldsymbol{\sigma}} \quad (3)$$

with Y the strain energy release rate density, $\boldsymbol{\epsilon}^e$ the elastic strain, $\tilde{\boldsymbol{\sigma}} = \boldsymbol{\sigma}/(1-D)$ the effective stress. According to the principle of strain equivalence (Lemaitre, 1971, Lemaitre and Chaboche, 1985, 1991) the elasticity law coupled with damage writes $\tilde{\boldsymbol{\sigma}} = \mathbf{E} : \boldsymbol{\epsilon}^e$ (with \mathbf{E} elasticity tensor of virgin material). The damage parameters are S , the damage strength, and s , the damage exponent. Damage law (3) leads then to a rate dependent ductility (Lemaitre and Desmorat, 2005, Besson, 2009b), but the higher the stress level the lower the ductility. Some authors prefer then to use—even in high strain rate visco-plasticity (Borvik et al, 2002)—the damage law

$$\dot{D} = AR_v^s \dot{p} H(p - p_D) \quad R_v = \frac{2}{3}(1 + \nu) + 3(1 - 2\nu) \left(\frac{\sigma_H}{\sigma_{eq}}\right)^2 \quad (4)$$

with R_v Lemaitre's triaxiality function, ν Poisson's ratio, A and s as damage parameters and where $H(x)$ is Heaviside function. This evolution law may be rewritten (Lemaitre and Chaboche, 1985,1991)

$$\dot{D} = \frac{R_v^s}{\epsilon_{pR} - p_D} \dot{p} H(p - p_D) \quad (5)$$

in order to make appear the accumulated plastic strain to rupture ϵ_{pR} and the damage threshold p_D , both identified in monotonic tension in Eq. (5).

Damage law (4) is in fact derived from a rate independent analysis with isotropic elasticity when the effective stress saturates at the ultimate stress σ_u , a material constant then, so that for $p \geq p_D$ (Lemaitre, 1992)

$$\dot{D} = \left(\frac{\bar{\sigma}_{eq}^2 R_v}{2ES} \right)^s \dot{p} \approx AR_v^s \dot{p} \quad \text{with} \quad A = \left(\frac{\sigma_u^2}{2ES} \right)^s \quad (6)$$

Setting A as a material parameter and using law $\dot{D} = AR_v^s \dot{p}$ —with $s = 0$ in (Borvik et al, 2002) recovering then Chu and Needleman (1980) nucleation term—for visco-plasticity coupled with damage analyses leads to a constant ductility independent from the loading rate (but dependent of the stress triaxiality for $s > 0$). This is the damage law that we propose next to generalize (with $s = 1$ for the sake of simplicity).

A possibility to account for the rate dependency exists, usually dedicated to dynamics and impact (Johnson and Cook, 1985): to enforce a zero damage threshold (this needs to make nonlinear the damage law) and to consider as rate dependent the damage parameter A (in an equivalent manner to make rate dependent the plastic strain to rupture ϵ_{pR} within Eq. (5)). This would make difficult the modeling of tertiary creep which may exhibit quite large strains to rupture ($> 0.1-0.2$) after a secondary creep stage at very low strain rate. Another possibility, used by Naumenko et al (2011), is to enforce an adequate stress dependency of the plastic strain to rupture ϵ_{pR} within damage law (5), the stress being rate dependent by the viscosity law. It is then very difficult to model both tertiary creep at different stress levels and monotonic tension at different strain rates. Naumenko et al (2011) mention that in monotonic tension the acceleration of the stress softening at high strains is then not reproduced (by taking $p_D = 0$ and by adding a strong nonlinearity of the damage evolution).

We propose in present work to gain a positive rate sensitivity of the ductility by introducing a rate dependent damage threshold p_D such as in Eq. (1) but formulated in an equivalent manner by means of a rate dependent threshold criterion f_D such as

$$f_D < 0 \quad \longrightarrow \quad D = 0 \quad (7)$$

We will formulate this threshold in the case of cubic material symmetry in Section 6.

4. Cubic elasticity from harmonic decomposition

In order to model the cubic anisotropy encountered for single crystal superalloys, such as CMSX-4, we now use the elasticity framework. We first present adequate mathematical tools: harmonic decomposition (Schouten, 1951, Backus, 1970, Spencer, 1970), Kelvin stresses and projectors (Kelvin, 1856, 1878, Rychlewski, 1984, Cowin et al, 1991, Biegler and Mehrabadi, 1995, François, 1995, Bertram and Olschewski, 1996, Arramon et al., 2000, Mahnken, 2002, Desmorat and Marull, 2011). We describe their use in continuum mechanics and define stress and plastic strain tensors dedicated to cubic material symmetry.

4.1. Cubic elasticity parameters

The three independent components of a cubic elasticity tensor \mathbb{E} (of components E_{ijkl} , having major and minor indicial symmetries $E_{ijkl} = E_{klij} = E_{jikl}$) are Young's modulus E , Poisson's ratio ν and the shear modulus $G \neq \frac{E}{2(1+\nu)}$, the bulk modulus being $K = \frac{E}{3(1-2\nu)}$.

In Natural Anisotropy Basis, the compliance tensor $\mathbb{S} = \mathbb{E}^{-1}$ ($S_{ijkl} = S_{klij} = S_{jikl}$) of a material having cubic material symmetry has for Kelvin matrix representation (Cowin and Mehrabadi, 1990)

$$[\mathbb{E}^{-1}] = \begin{bmatrix} \frac{1}{E} & -\frac{\nu}{E} & -\frac{\nu}{E} & 0 & 0 & 0 \\ -\frac{\nu}{E} & \frac{1}{E} & -\frac{\nu}{E} & 0 & 0 & 0 \\ -\frac{\nu}{E} & -\frac{\nu}{E} & \frac{1}{E} & 0 & 0 & 0 \\ 0 & 0 & 0 & \frac{1}{2G} & 0 & 0 \\ 0 & 0 & 0 & 0 & \frac{1}{2G} & 0 \\ 0 & 0 & 0 & 0 & 0 & \frac{1}{2G} \end{bmatrix}_{NAB} \quad (8)$$

according to

$$\begin{cases} E_{1111} = E_{2222} = E_{3333} = \frac{(1-\nu)E}{1-\nu-2\nu^2} \\ E_{1122} = E_{1133} = E_{2233} = \frac{\nu E}{1-\nu-2\nu^2} \\ E_{1212} = E_{1313} = E_{2323} = G \end{cases} \quad (9)$$

The other E_{ijkl} are either obtained from the indicial symmetries or are equal to zero.

4.2. Harmonic decomposition of cubic elasticity tensor

An elasticity tensor \mathbb{E} belonging to the cubic symmetry class can be recast as

$$\mathbb{E} = 2\mu\mathbb{I} + \lambda\mathbf{1} \otimes \mathbf{1} + \mathbb{H}, \quad \text{tr}_{12}\mathbb{H} = \text{tr}_{13}\mathbb{H} = 0 \quad (10)$$

with \mathbb{I} the fourth order unit tensor. Eq. (10) is the harmonic decomposition of \mathbb{E} cubic (Backus, 1970, Cowin et al, 1991, Baerheim, 1993, Forte and Vianello, 1996). Generalized Lamé constants $\lambda = \lambda(\mathbb{E}), \mu = \mu(\mathbb{E})$ are two invariants of the elasticity tensor. Fourth order harmonic part $\mathbb{H} = \mathbb{H}(\mathbb{E})$ is uniquely defined (Backus, 1970). It is both

- totally symmetric: having the major and minor indicial symmetries of the elasticity tensor and the additional Cauchy symmetry $H_{ijkl} = H_{ikjl}$,
- traceless: $(\text{tr}_{12}\mathbb{H})_{ij} = H_{kkij} = (\text{tr}_{13}\mathbb{H})_{ij} = H_{kikj} = 0$.

More precisely, λ, μ are functions of the invariants $\text{tr}(\text{tr}_{12}\mathbb{E})$ and $\text{tr}(\text{tr}_{13}\mathbb{E})$,

$$\lambda = \frac{1}{15}(2 \text{tr}(\text{tr}_{12}\mathbb{E}) - \text{tr}(\text{tr}_{13}\mathbb{E})) \quad (11)$$

$$\mu = \frac{1}{30}(-\text{tr}(\text{tr}_{12}\mathbb{E}) + 3 \text{tr}(\text{tr}_{13}\mathbb{E})) \quad (12)$$

The fourth order harmonic part \mathbb{H} is then

$$\mathbb{H} = \mathbb{E} - 2\mu\mathbb{I} - \lambda\mathbf{1} \otimes \mathbf{1} \quad (13)$$

A third (rational) invariant of elasticity tensor \mathbb{E} belonging to cubic symmetry class is material constant δ which is defined as (Auffray et al (2014), Section 5.1)

$$\delta = \frac{J_3}{4J_2} = \frac{\text{tr}(\text{tr}_{13}\mathbb{H}^3)}{4 \text{tr}(\text{tr}_{13}\mathbb{H}^2)} \quad (14)$$

where

$$J_2 = \text{tr}(\text{tr}_{13}\mathbb{H}^2) = \|\mathbb{H}\|^2 = H_{ijkl}H_{ijkl}, \quad J_3 = \text{tr}(\text{tr}_{13}\mathbb{H}^3) = H_{ijkl}H_{klpq}H_{pqij} \quad (15)$$

are the first two polynomial invariants of \mathbb{H} after Boehler et al (1994) (here $J_2 = 480\delta^2$ and $J_3 = 1920\delta^3$). Note that Olive et al (2017a) give the minimal integrity basis made of 297 polynomial invariants for elasticity tensor (whatever its symmetry class).

4.3. Kelvin stresses – Kelvin projectors

A cubic elasticity tensor \mathbb{E} and, in an equivalent manner, its invert \mathbb{E}^{-1} have three eigentensors: the hydrostatic stress tensor σ^H , and two deviatoric stress tensors σ^d and $\sigma^{\bar{d}}$ (σ^d diagonal in Natural Anisotropy Basis, deviatoric, $\sigma^{\bar{d}}$ out-of-diagonal in this basis, also deviatoric), such as

$$\mathbb{E} : \sigma^H = \frac{E}{1-2\nu}\sigma^H, \quad \mathbb{E} : \sigma^d = \frac{E}{1+\nu}\sigma^d, \quad \mathbb{E} : \sigma^{\bar{d}} = 2G\sigma^{\bar{d}} \quad (16)$$

with the orthogonality properties $\sigma^d : \sigma^H = \sigma^{\bar{d}} : \sigma^H = \sigma^d : \sigma^{\bar{d}} = 0$ and the deviatoric and total stresses partitions (Bertram and Olschewski, 1996)

$$\sigma' = \sigma^d + \sigma^{\bar{d}} \quad \text{and} \quad \sigma = \sigma^d + \sigma^{\bar{d}} + \sigma^H \quad (17)$$

Such partitions are objective —*i.e.* frame invariant— in case of cubic material symmetry.

The second order tensors σ^H, σ^d and $\sigma^{\bar{d}}$ are the so-called Kelvin stresses, associated with Kelvin moduli $\frac{E}{1-2\nu} = 3K, \frac{E}{1+\nu}$ and $2G$ (the three eigenvalues of \mathbb{E} , Kelvin (1856, 1878), Cowin et al (1991)). They are obtained thanks to Kelvin fourth order projectors $\mathbb{P}^H, \mathbb{P}^d, \mathbb{P}^{\bar{d}}$ (François, 1995),

$$\begin{aligned} \mathbb{P}^H : \sigma &= \sigma^H = \frac{1}{3} \text{tr} \sigma \mathbf{1} \\ \mathbb{P}^d : \sigma &= \sigma^d \\ \mathbb{P}^{\bar{d}} : \sigma &= \sigma^{\bar{d}} \end{aligned} \quad (18)$$

with $\mathbb{P}^H = \frac{1}{3} \mathbf{1} \otimes \mathbf{1}$ standard hydrostatic projector. The two other projectors can be build directly from the harmonic part $\mathbb{H} = \mathbb{E} - 2\mu\mathbb{I} - \lambda\mathbf{1} \otimes \mathbf{1}$ of cubic elasticity tensor as

$$\mathbb{P}^d = \frac{1}{5} \left(\mathbb{J} + \frac{\mathbb{H}}{\mu - G} \right), \quad \mathbb{P}^{\bar{d}} = \mathbb{J} - \mathbb{P}^d, \quad \mathbb{J} = \mathbb{I} - \frac{1}{3} \mathbf{1} \otimes \mathbf{1} \quad (19)$$

with $\mu \neq G$ and $\mathbb{H} \neq \mathbf{0}$ for cubic symmetry class (see Appendix A) and $\mathbb{P}^H + \mathbb{P}^d + \mathbb{P}^{\bar{d}} = \mathbb{I}$.

To get the projectors \mathbb{P}^d and $\mathbb{P}^{\bar{d}}$ we only have to use Eq. (19) with rational invariant $\mu - G = 4\delta = \text{tr}(\text{tr}_{13} \mathbb{H}^3) / \text{tr}(\text{tr}_{13} \mathbb{H}^2)$ (Eq. (14)-(82)) easily computed in any working basis and with \mathbb{H} given by linear relationship $\mathbb{H} = \mathbb{E} - 2\mu\mathbb{I} - \lambda\mathbf{1} \otimes \mathbf{1}$ with λ, μ from (11)-(12). Present determination of the Kelvin projectors does not need to solve the characteristic polynomial nor to find the eigenvectors of $[\mathbb{E}]$.

The Kelvin stresses can be used to particularize Hill equivalent stress to cubic symmetry as writing in Natural Anisotropy Basis

$$\sigma_{\text{Hill}} = \sqrt{\frac{1}{2} \left((\sigma_{11} - \sigma_{22})^2 + (\sigma_{22} - \sigma_{33})^2 + (\sigma_{33} - \sigma_{11})^2 \right) + \frac{3}{2} h^2 \left(\sigma_{12}^2 + \sigma_{21}^2 + \sigma_{13}^2 + \sigma_{31}^2 + \sigma_{23}^2 + \sigma_{32}^2 \right)} \quad (20)$$

is equivalent to intrinsic writing

$$\sigma_{\text{Hill}} = \sqrt{\frac{3}{2} \left(\boldsymbol{\sigma}^d : \boldsymbol{\sigma}^d + h^2 \boldsymbol{\sigma}^{\bar{d}} : \boldsymbol{\sigma}^{\bar{d}} \right)} = \sqrt{(\boldsymbol{\sigma}^d)_{eq}^2 + h^2 (\boldsymbol{\sigma}^{\bar{d}})_{eq}^2} \quad (21)$$

with h a material parameter ($h = 1$ for isotropy, standard von Mises stress σ_{eq} then recovered).

The notations $\boldsymbol{\sigma}_{eq}^d, \boldsymbol{\sigma}_{eq}^{\bar{d}}$ are used next for the following norms of deviatoric stress tensors $\boldsymbol{\sigma}^d, \boldsymbol{\sigma}^{\bar{d}}$,

$$\boldsymbol{\sigma}_{eq}^d = (\boldsymbol{\sigma}^d)_{eq} = \sqrt{\frac{3}{2} \boldsymbol{\sigma}^d : \boldsymbol{\sigma}^d}, \quad \boldsymbol{\sigma}_{eq}^{\bar{d}} = (\boldsymbol{\sigma}^{\bar{d}})_{eq} = \sqrt{\frac{3}{2} \boldsymbol{\sigma}^{\bar{d}} : \boldsymbol{\sigma}^{\bar{d}}} \quad (22)$$

with in Natural Anisotropy Basis

$$\begin{cases} \boldsymbol{\sigma}_{eq}^d = \sqrt{\frac{1}{2} \left[(\sigma_{11} - \sigma_{22})^2 + (\sigma_{22} - \sigma_{33})^2 + (\sigma_{33} - \sigma_{11})^2 \right]} \\ \boldsymbol{\sigma}_{eq}^{\bar{d}} = \sqrt{\frac{3}{2} \left[\sigma_{12}^2 + \sigma_{21}^2 + \sigma_{23}^2 + \sigma_{32}^2 + \sigma_{31}^2 + \sigma_{13}^2 \right]} \end{cases} \quad (23)$$

Note that von Mises equivalent stress σ_{eq} is limiting case $h = 1$ in (20)-(21), *i.e.*

$$\sigma_{eq} = \sqrt{\frac{3}{2} \boldsymbol{\sigma}' : \boldsymbol{\sigma}'} = \sqrt{(\boldsymbol{\sigma}^d)_{eq}^2 + (\boldsymbol{\sigma}^{\bar{d}})_{eq}^2} \quad (24)$$

with $\boldsymbol{\sigma}' = \boldsymbol{\sigma} - \frac{1}{3} \text{tr} \boldsymbol{\sigma} \mathbf{1}$ usual deviatoric part of stress tensor.

The non quadratic norm for cubic materials (expressed in Natural Anisotropy Basis, Desmorat et al (2017))

$$\|\boldsymbol{\sigma}^{\bar{d}}\|_a = 3 \left(\frac{|\sigma_{12}|^a + |\sigma_{21}|^a + |\sigma_{13}|^a + |\sigma_{31}|^a + |\sigma_{23}|^a + |\sigma_{32}|^a}{6} \right)^{1/a} \quad (25)$$

is a generalization of equivalent stress $\boldsymbol{\sigma}_{eq}^{\bar{d}}$ such as *i)* $\boldsymbol{\sigma}_{eq}^{\bar{d}} = \|\boldsymbol{\sigma}^{\bar{d}}\|_{a=2}$, *ii)* $\|\boldsymbol{\sigma}^{\bar{d}}\|_a = 0$ for tension in orientation $\langle 001 \rangle$ and *iii)* $\|\boldsymbol{\sigma}^{\bar{d}}\|_a = \sigma$ for tension in orientation $\langle 111 \rangle$.

4.4. Plastic strains dedicated to cubic symmetry from Kelvin projectors

The Kelvin projectors allow to define different strain tensors (total, elastic and plastic) dedicated to cubic symmetry class (Biegler and Mehrabadi, 1995, François, 1995, Bertram and Olschewski, 1996, Desmorat and Marull, 2011). When applied to the —here deviatoric— plastic strain tensor they define for cubic symmetry two deviatoric tensors $\boldsymbol{\epsilon}^{pd}$ and $\boldsymbol{\epsilon}^{p\bar{d}}$ as

$$\boldsymbol{\epsilon}^{pd} = \mathbb{P}^d : \boldsymbol{\epsilon}^p \quad \text{and} \quad \boldsymbol{\epsilon}^{p\bar{d}} = \mathbb{P}^{\bar{d}} : \boldsymbol{\epsilon}^p \quad (26)$$

such as the partition $\boldsymbol{\epsilon}^p = \boldsymbol{\epsilon}^{pd} + \boldsymbol{\epsilon}^{p\bar{d}}$ is frame invariant for cubic symmetry class. In such a plastic strain partition $\boldsymbol{\epsilon}^{pd}$ is the diagonal part of $\boldsymbol{\epsilon}^p$ in Natural Anisotropy Basis, $\boldsymbol{\epsilon}^{p\bar{d}}$ is the out-of-diagonal part of $\boldsymbol{\epsilon}^p$ in this basis, with the orthogonality property $\boldsymbol{\epsilon}^{pd} : \boldsymbol{\epsilon}^{p\bar{d}} = 0$.

From these two plastic strain tensors, one defines two accumulated plastic strains (Desmorat and Marull, 2011), one (p^d) associated to the "deviatoric diagonal" Kelvin mode, another to the "deviatoric out of diagonal" Kelvin mode ($p^{\bar{d}}$)

$$p^d = \int \sqrt{\frac{2}{3} \dot{\boldsymbol{\epsilon}}^{pd} : \dot{\boldsymbol{\epsilon}}^{pd}} dt \quad \text{and} \quad p^{\bar{d}} = \int \sqrt{\frac{2}{3} \dot{\boldsymbol{\epsilon}}^{p\bar{d}} : \dot{\boldsymbol{\epsilon}}^{p\bar{d}}} dt \quad (27)$$

Usual (isotropic) accumulated plastic strain $p = \int \sqrt{\frac{2}{3} \dot{\boldsymbol{\epsilon}}^p : \dot{\boldsymbol{\epsilon}}^p} dt$ is such as

$$\dot{p} = \sqrt{(\dot{p}^d)^2 + (\dot{p}^{\bar{d}})^2} \quad (28)$$

4.5. Stresses and plastic strains for tensions along $\langle 001 \rangle$ and along $\langle 111 \rangle$

The Kelvin stresses and strains decouple the constitutive equations for two particular loading often used for the identification of crystal (visco-)plasticity of cubic superalloys (uniaxial loading in orientations $\langle 001 \rangle$ and $\langle 111 \rangle$):

- $\sigma^d = \sigma'$, $\sigma^{\bar{d}} = \mathbf{0}$, $\epsilon^{pd} = \epsilon^p$ and $\epsilon^{p\bar{d}} = \mathbf{0}$ for tension along $\langle 001 \rangle$, for which $(\sigma^d)_{eq} = \sigma_{eq} = \sigma$, $p^d = p$, $p^{\bar{d}} = 0$.
- $\sigma^d = \mathbf{0}$, $\sigma^{\bar{d}} = \sigma'$, $\epsilon^{p\bar{d}} = \epsilon^p$ and $\epsilon^{pd} = \mathbf{0}$ for tension along $\langle 111 \rangle$, for which $(\sigma^{\bar{d}})_{eq} = \sigma_{eq} = \sigma$, $p^d = 0$, $p^{\bar{d}} = p$.

This decoupling allows to represent independently —*i.e.* with two different subsets of material parameters— by a single multiaxial model the uniaxial responses of cubic superalloys both in crystallographic orientation $\langle 001 \rangle$ and in orientation $\langle 111 \rangle$ (Desmorat and Marull, 2011). The material parameters for orientation $\langle 111 \rangle$ will be next overlined. For example if σ_y , K_N , N , ϵ_{pD}^0 , B , \dot{p}_0 , A are material parameters for orientation $\langle 001 \rangle$, the parameters (having the same role) for orientation $\langle 111 \rangle$ will be denoted $\bar{\sigma}_y$, \bar{K}_N , \bar{N} , $\bar{\epsilon}_{pD}^0$, \bar{B} , $\bar{\dot{p}}_0$, \bar{A} .

5. Thermodynamics of coupling cubic elasticity / isotropic damage

We consider Lemaitre and Chaboche (1985,1991) thermodynamics framework for isotropic damage. We furthermore use the Kelvin mode based formulation of François (1995), but with a single scalar damage variable D . The hardening and the coupling with microstructural changes are here neglected. The Gibbs enthalpy density for cubic material, function of the stress tensor σ , of the plastic strain tensor ϵ^p and of the damage D , is

$$\rho\psi^* = \frac{1+\nu}{2E(1-D)}\sigma^d : \sigma^d + \frac{1}{4G(1-D)}\sigma^{\bar{d}} : \sigma^{\bar{d}} + \frac{\langle \text{tr } \sigma \rangle_+^2}{18K(1-D)} + \frac{\langle \text{tr } \sigma \rangle_-^2}{18K} + \sigma : \epsilon^p \quad (29)$$

with ρ the density, and where it is assumed that the damage does not affect the bulk modulus $K = E/3(1-2\nu)$ at negative hydrostatic stress $\sigma_H = \frac{1}{3} \text{tr } \sigma$. The notations $\langle x \rangle_+ = \max(0, x)$ and $\langle x \rangle_- = \min(0, x)$ denote respectively the positive and negative parts of scalar x . The state potential is convex with respect to both variables σ and D .

5.1. State laws – Effective stress and triaxiality function

The elasticity law writes then

$$\epsilon = \rho \frac{\partial \psi^*}{\partial \sigma} \quad (30)$$

which is equivalent to

$$\epsilon^e = \frac{1+\nu}{E}\tilde{\sigma}^d + \frac{1}{2G}\tilde{\sigma}^{\bar{d}} + \frac{1-2\nu}{3E} \text{tr } \tilde{\sigma} \mathbf{1} = \mathbb{E}^{-1} : \tilde{\sigma} \quad (31)$$

with $\epsilon^e = \epsilon - \epsilon^p$ the elastic strain. Fourth order tensor \mathbb{E} is Hooke's tensor of virgin (cubic) material. Eq. (30) defines the effective stress

$$\tilde{\sigma} = \frac{\sigma'}{1-D} + \frac{1}{3} \left[\frac{\langle \text{tr } \sigma \rangle_+}{1-D} + \langle \text{tr } \sigma \rangle_- \right] \mathbf{1} \quad (32)$$

which is symmetric and independent from the elasticity parameters. We have set

$$\tilde{\sigma}^d = \mathbb{P}^d : \tilde{\sigma}, \quad \tilde{\sigma}^{\bar{d}} = \mathbb{P}^{\bar{d}} : \tilde{\sigma} \quad (33)$$

At positive hydrostatic stress Eq. (32) recovers standard definition $\tilde{\sigma} = \sigma/(1-D)$. A partial stiffness recovery due to microcracks closure at negative hydrostatic stresses is modeled.

The strain energy release rate density writes:

$$Y = \rho \frac{\partial \psi^*}{\partial D} = \frac{1+\nu}{2E}\tilde{\sigma}^d : \tilde{\sigma}^d + \frac{1}{4G}\tilde{\sigma}^{\bar{d}} : \tilde{\sigma}^{\bar{d}} + \frac{1}{18K}\langle \text{tr } \tilde{\sigma} \rangle_+^2 \quad (34)$$

where $\tilde{\sigma}^d = \mathbb{P}^d : \tilde{\sigma}$ and $\tilde{\sigma}^{\bar{d}} = \mathbb{P}^{\bar{d}} : \tilde{\sigma}$ so that

$$Y = \frac{\tilde{\sigma}_{\text{Hill}}^2}{2E} R_v \geq 0 \quad R_v = \frac{2}{3}(1+\nu) \left(\frac{\sigma_{eq}^d}{\sigma_{\text{Hill}}} \right)^2 + \frac{E}{3G} \left(\frac{\sigma_{eq}^{\bar{d}}}{\sigma_{\text{Hill}}} \right)^2 + 3(1-2\nu) \left\langle \frac{\sigma_H}{\sigma_{\text{Hill}}} \right\rangle_+^2 \quad (35)$$

in which cubic Hill equivalent stress (20)-(21) has been introduced. Triaxiality function R_v extends to cubic material symmetry the isotropic definition (4) of (Lemaitre and Chaboche, 1985,1991, Lemaitre, 1992). Isotropy ($G = E/2(1+\nu)$ and Hill's parameter $h = 1$) gives back $R_v = 1$ for uniaxial tension performed in any direction.

For an uniaxial stress state in crystallographic direction $\langle 001 \rangle$:

$$\begin{cases} R_v = 1 & \text{if } \sigma > 0 \\ R_v = \frac{2}{3}(1+\nu) & \text{if } \sigma < 0 \end{cases} \quad (36)$$

For an uniaxial stress state in crystallographic direction $\langle 111 \rangle$:

$$\begin{cases} R_v = \frac{1}{3h^2} \left[\frac{E}{G} + 1 - 2\nu \right] & \text{if } \sigma > 0 \\ R_v = \frac{E}{3h^2 G} & \text{if } \sigma < 0 \end{cases} \quad (37)$$

We set

$$R_v^{(111)} = \frac{1}{3h^2} \left[\frac{E}{G} + 1 - 2\nu \right] \quad (38)$$

5.2. Positivity of intrinsic dissipation

The intrinsic dissipation due to visco-plasticity coupled with damage is, in present case without hardening (Lemaitre and Chaboche, 1985,1991)

$$\mathcal{D}_0 = \boldsymbol{\sigma} : \dot{\boldsymbol{\epsilon}}^p + Y\dot{D} \quad (39)$$

If furthermore the plastic strain is split in two, setting

$$\boldsymbol{\epsilon}^p = \boldsymbol{\epsilon}_1^p + \boldsymbol{\epsilon}_2^p \quad (40)$$

and the associated normality rules are written

$$\dot{\boldsymbol{\epsilon}}_\alpha^p = \dot{r}_\alpha \frac{\partial f_\alpha}{\partial \boldsymbol{\sigma}} = \frac{\dot{r}_\alpha}{1-D} \frac{\partial f_\alpha}{\partial \tilde{\boldsymbol{\sigma}}}, \quad \alpha = 1, 2 \quad (\text{no sum}) \quad (41)$$

with two criterion functions $f_\alpha = f_\alpha(\tilde{\boldsymbol{\sigma}}')$ convex in the deviatoric effective stress $\tilde{\boldsymbol{\sigma}}' = \boldsymbol{\sigma}'/(1-D)$ (according to Eq. (32)) and two visco-plastic multipliers \dot{r}_α . Examples for cubic single crystals are $f_1 = \tilde{\sigma}_{\text{Hill}} - \sigma_y$ and $f_2 = \tilde{\sigma}_{eq}^{\bar{d}} - \bar{\sigma}_y$ or $f_2 = \|\tilde{\boldsymbol{\sigma}}^{\bar{d}}\|_a - \bar{\sigma}_y$ (Eq. (25)), which make appear as material parameters the yield stresses $\sigma_y, \bar{\sigma}_y$ respectively in directions $\langle 001 \rangle$ and $\langle 111 \rangle$. The plastic strains rates $\dot{\boldsymbol{\epsilon}}_\alpha^p$ are then deviatoric (so is $\boldsymbol{\epsilon}^p$, considered visco-plasticity is incompressible) and

$$\mathcal{D}_0 = \dot{r}_1 \tilde{\boldsymbol{\sigma}} : \frac{\partial f_1}{\partial \tilde{\boldsymbol{\sigma}}} + \dot{r}_2 \tilde{\boldsymbol{\sigma}} : \frac{\partial f_2}{\partial \tilde{\boldsymbol{\sigma}}} + Y\dot{D} \quad (42)$$

The terms $\tilde{\boldsymbol{\sigma}} : \partial f_\alpha / \partial \tilde{\boldsymbol{\sigma}}$ are positive by convexity (Halphen and Nguyen, 1975). The strain energy release rate Y , given by Eq. (34), is positive. Simply enforcing positive visco-plastic multipliers $\dot{r}_\alpha \geq 0$ and damage rate $\dot{D} \geq 0$ by adequate viscosity and damage evolution laws implies the positivity of the intrinsic dissipation

$$\mathcal{D}_0 \geq 0 \quad (43)$$

for any loading case.

6. Damage threshold and evolution law for cubic symmetry class

Let us use the decoupling of the mechanical responses obtained for orientations $\langle 001 \rangle$ and $\langle 111 \rangle$ when accumulated plastic strains $p^{\bar{d}}$ and p^d are introduced within visco-plasticity coupled with damage constitutive equations.

6.1. Rate dependent damage threshold for cubic material symmetry

We define for cubic materials the dimensionless equivalent visco-plastic strain \hat{P} as

$$\hat{P} = \sup_t \left[\frac{p^d}{\epsilon_{pD}^0} \exp \left(-B \left\langle 1 - \frac{\dot{p}_0}{\dot{p}^d} \right\rangle \right) + \frac{p^{\bar{d}}}{\epsilon_{pD}^{\bar{d}}} \exp \left(-\bar{B} \left\langle 1 - \frac{\dot{p}_0^{\bar{d}}}{\dot{p}^{\bar{d}}} \right\rangle \right) \right] \quad (44)$$

The damage threshold criterion is expressed as

$$f_D = \hat{P} - 1 \quad (45)$$

and satisfies (7), *i.e.* $f_D < 0 \rightarrow$ no damage growth, $f_D \geq 0 \rightarrow$ damage growth by considered damage evolution law.

Even if we have in mind applications with monotonic loading mainly, due to the supremum over time in Eq. (44), the scalar \hat{P} behaves as a dimensionless accumulated plastic strain (it is positive monotonic, $\hat{P} \geq 0$, $\frac{d\hat{P}}{dt} \geq 0$), but rate dependent. Due to this feature, once the damage threshold has been reached the damage variable D always grows in visco-plasticity stages (*i.e.* when $\dot{p} > 0$), as in original Lemaitre's damage model (Lemaitre (1984, 1992), with $\dot{D} = 0$ in the elastic loading-unloading stages only). We expect that Eq. (45) can be used for cyclic loading also. But recall that in that case, an accurate damage modeling of the creep-fatigue interaction needs kinematic hardening (Sermage, 1998, Sermage et al, 2000), which is not considered in present work.

We have then the following main two practical particular cases, for which the condition $\hat{P} \geq 1 \rightarrow \dot{D} > 0$ simplifies:

- case of monotonic tension (including creep) in orientation $\langle 001 \rangle$: $p^d = p = \epsilon_p$, $p^{\bar{d}} = 0$, so that in such an uniaxial case writing $f_D \geq 0 \rightarrow \dot{D} > 0$ gives

$$p \geq p_D^{\langle 001 \rangle}(\dot{p}) = \epsilon_{pD}^0 \exp\left(B\left\langle 1 - \frac{\dot{p}_0}{\dot{p}} \right\rangle\right) \rightarrow \dot{D} > 0 \quad (46)$$

- case of monotonic tension (including creep) in orientation $\langle 111 \rangle$: $p^d = 0$, $p^{\bar{d}} = p = \epsilon_p$ so that in such a case to write $f_D \geq 0 \rightarrow \dot{D} > 0$ gives

$$p \geq p_D^{\langle 111 \rangle}(\dot{p}) = \bar{\epsilon}_{pD}^0 \exp\left(\bar{B}\left\langle 1 - \frac{\dot{p}_0}{\dot{p}} \right\rangle\right) \rightarrow \dot{D} > 0 \quad (47)$$

The material parameters ϵ_{pD}^0 , B , \dot{p}_0 , are then those of the damage threshold rate dependency measured in direction $\langle 001 \rangle$ (monotonic loading, Fig. 7). The material parameters $\bar{\epsilon}_{pD}^0$, \bar{B} , \dot{p}_0 , are those of the damage threshold rate dependency measured in direction $\langle 111 \rangle$ (Fig. 8).

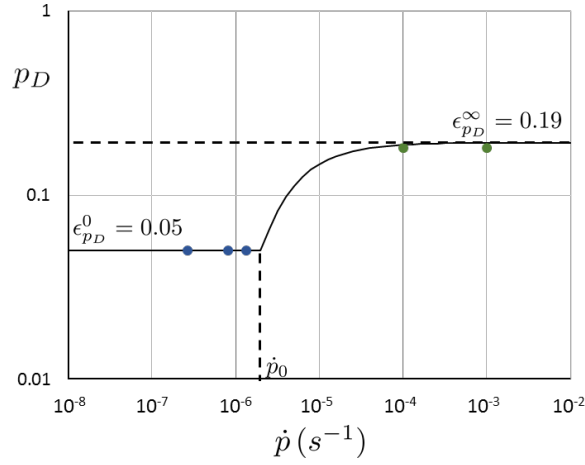


Figure 7: Damage threshold p_D as a function of the accumulated plastic strain rate \dot{p} for $\langle 001 \rangle$ CMSX-4 (bullets: experiments, solid line: Eq. (46)).

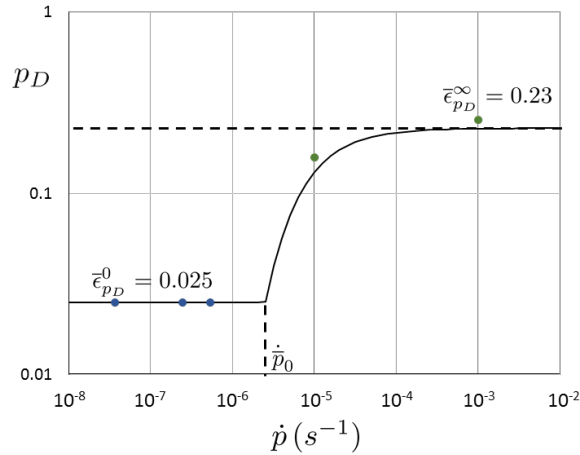


Figure 8: Damage threshold p_D as a function of the accumulated plastic strain rate \dot{p} for $\langle 111 \rangle$ CMSX-4 (bullets: experiments, solid line: Eq. (47)).

In order to determine the damage growth condition for the other crystallographic orientations or for multiaxial loading simply apply criterion (44)-(45) with p^d and $p^{\bar{d}}$ defined by Eq. (26)-(27).

6.2. Damage evolution law for cubic material symmetry

We now extend the damage law $\dot{D} = AR_v \dot{p}$ to cubic material symmetry as :

$$\dot{D} = R_v \left(A \dot{p}^d + \bar{A} \dot{p}^{\bar{d}} + A_{\text{dis}} \sqrt{\dot{p}^d \dot{p}^{\bar{d}}} \right) H(f_D) \quad (48)$$

with Heaviside function $H(x)$ such as $H(x) = 0$ for $x < 0$ and $H(x) = 1$ for $x \geq 0$ and previous threshold function f_D (Eq. (44)-(45)). Eq. (48) satisfies $f_D < 0 \rightarrow$ no damage, $f_D \geq 0 \rightarrow$ damage increase.

When introduced, the additional damage parameter A_{dis} induces a faster damage increase for loadings not aligned with the $\langle 001 \rangle$ and $\langle 111 \rangle$ directions. The extra term $A_{\text{dis}}(\dot{p}^d \dot{p}^{\bar{d}})^{1/2}$ vanishes $\forall A_{\text{dis}}$ in uniaxial loading performed either in crystallographic orientation $\langle 001 \rangle$ or in orientation $\langle 111 \rangle$.

As for original Rice & Tracey's, Gurson's and Lemaitre's laws, the damage evolution law (48) does not introduce a strain rate dependency by itself: \dot{p}^d , $\dot{p}^{\bar{d}}$ and $(\dot{p}^d \dot{p}^{\bar{d}})^{1/2}$ are all homogeneous to s^{-1} , i.e. to \dot{p} (Eq. (49)).

$$dD = R_v (A dp^d + \bar{A} dp^{\bar{d}} + A_{\text{dis}} \sqrt{dp^d dp^{\bar{d}}}) H(f_D) \quad (49)$$

Cubic triaxiality function R_v is defined in Eq. (35). We have then the main two practical particular cases:

- for monotonic tension (including creep) in orientation $\langle 001 \rangle$: $R_v = 1$, $p^d = p = \epsilon_p$, $p^{\bar{d}} = 0$ and

$$\dot{D} = A \dot{p} H(p - p_D^{(001)}(\dot{p})) \quad (50)$$

- for monotonic tension (including creep) in orientation $\langle 111 \rangle$: $R_v = R_v^{(111)} = \text{const}$ (given by Eq. (38)), $p^d = 0$, $p^{\bar{d}} = p = \epsilon_p$ and

$$\dot{D} = \bar{A} R_v^{(111)} \dot{p} H(p - p_D^{(111)}(\dot{p})) \quad (51)$$

They exhibit anisotropy of the damage growth when $\bar{A} R_v^{(111)} \neq A$. The damage threshold functions $p_D^{(001)}(\dot{p})$ and $p_D^{(111)}(\dot{p})$ are given by Eq. (46)-(47)

The curves damage D versus accumulated plastic strain p obtained for monotonic tension of CMSX-4 along the $\langle 111 \rangle$ direction are plotted in Fig. 9 (with then $p = p^{\bar{d}}$). A critical damage $D_c = 0.15$ is assumed in order to recover the observed (experimental) time to rupture (t_r) when performing gauss point simulation (anticipating Fig. 15). For the structural computations, we will allow for the strain localization phenomenon to take place by setting a large value for critical damage, $D_c = 0.999$. The damage parameters are: $\epsilon_{pD}^0 = 0.05$, $\bar{\epsilon}_{pD}^0 = 0.025$, $\dot{p}_0 = 210^{-6} s^{-1}$, $\bar{p}_0 = 2.510^{-6} s^{-1}$, $B = 1.35$, $\bar{B} = 2.21$, $A = 2.8$, $\bar{A} R_v^{(111)} = 2.5$, $A_{\text{dis}} = 0$. The slopes of the curves are independent from the loading rate (but they differ, equal to A for $\langle 001 \rangle$ and to \bar{A} for $\langle 111 \rangle$). The experiments are plotted thanks to the plateaux σ_{plateau} of the curves of Fig. 3 for $\langle 111 \rangle$ orientation using formula $D^{\text{exp}} = 1 - \sigma_{\text{plateau}}/\sigma$ (Lemaitre, 1992). The increase of ductility with $\dot{\epsilon}$ is attributed to the rate dependent damage threshold. The corresponding stress-strain curves are those of Fig. 12.

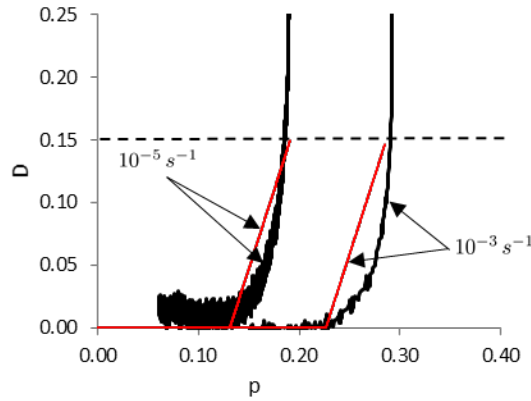


Figure 9: $D(p)$ curves in monotonic tension at different strain rates up to critical damage $D_c = 0.15$ (CMSX-4 at 1050°C, $\langle 111 \rangle$ crystallographic orientation).

7. Full damage model with microstructure degradation and rate dependent threshold

In order to obtain a close link with Schmid based single crystal visco-plasticity (Schmid and Boas, 1935, Hill and Rice, 1972, Rice, 1975, Asaro, 1983, Peirce et al., 1983, Asaro and Lubarda, 2006, Altenbach and Kruch, 2013), multi-criterion by nature, a two criterion framework inspired from (Cowin et al, 1991, Bertram and Olschewski, 1996, Mahnken, 2002) has been used by Desmorat et al (2017) and applied to CMSX-4 single crystal superalloy. It allows for the modeling of visco-plasticity coupled with microstructure degradation (without "mechanical" damage D in previous work). The material parameters of this initial model are kept, they are those for CMSX-4 at 1050°C given in (Desmorat et al, 2017) (see Appendix D).

We follow next a physically based approach dedicated to single crystals, the coupling visco-plasticity / microstructure degradation being represented by an Orowan macroscopic stress (Fedelich et al, 2009, Cormier and Cailletaud, 2010a, Staroselsky et al, 2008, 2011, Fedelich et al, 2012b). Such constitutive equations have sometimes been coupled to continuous damage (Tinga et al, 2009b, Ghighi et al, 2012, le Graverend et al, 2014a). These microstructure sensitive approaches coupled with damage, and also the micromorphic approach of Aslan et al (2011) and the damage models of Kaminski (2007) and Marull and Desmorat (2013), for single crystals still, did not model the ductility in monotonic tension. In a complementary point of view for initially isotropic materials, note that Besseling and van der Giessen (1994) and Naumenko et al (2011) characterize high temperature hardening and recovery —and softening processes by continuous damage for the second authors— by a two phase composite model with creep-hard and creep-soft constituents, representative of the coarsening of subgrain structure: in second work on X20CrMoV12-1 steel at 600°C, the volume fraction of the creep-hard constituent is assumed to decrease toward a saturation value by means of a macroscopic evolution law. The generalization to cubic symmetry of these authors hardening rules and associated constitutive equations for primary creep is left to further work.

We now couple the initial model of Desmorat et al (2017) to damage by means of the principle of strain equivalence (Lemaitre, 1971): the stress in the elasticity law as well as in criterion functions is replaced by the effective stress (32) and damage evolution law (48) is considered with rate dependent threshold (44)-(45). The hardening is neglected at considered temperature. Considered damage modeling approach is not formulated at the slip system scale and is hence not directly driven by plastic activity on slip systems.

7.1. Tensorial γ channel width variables \mathbf{w} and ω

The effect of the microstructure change/degradation has not to be mistaken with mechanical damage D , representative of the microcracks and voids present within RVE of Continuum Mechanics. Rafting phenomenon is represented by a tensorial variable: the γ channel width second order (symmetric) tensor \mathbf{w} , of initial value $\mathbf{w}(t=0) = w_0 \mathbf{1}$ (i.e. $w_{ij}(t) = w_0 \delta_{ij}$ in terms of components, eigenvalues denoted w_i in Fig. 6). We have $w_0 \approx 80$ nm for CMSX-4 at 1050°C. Such an initial value $w_0 = w_0(f_\gamma(T))$ is temperature dependent through the change of γ' volume fraction with $f_\gamma \approx 0.7$ at room temperature, $f_\gamma \approx 0.55$ at 1050°C (Roebuck et al, 2001, Fedelich et al, 2012b, Desmorat et al, 2017). The mechanical effect of the microstructure degradation is quantified by macroscopic Orowan stress, inversely proportional to the norm $\|\mathbf{w}\| = \sqrt{\mathbf{w} : \mathbf{w}}$ of γ channel width tensor. This is therefore inversely proportional to the norm of dimensionless tensor $\omega = \mathbf{w}/w_0$, taken as a state variable of thermodynamics

$$\sigma_{\text{ORO}} = \frac{\kappa_{\text{ORO}} G}{\|\omega\|} \quad \omega = \frac{\mathbf{w}}{w_0} \quad (52)$$

with κ_{ORO} a material parameter and G the shear modulus. The model is completed by an evolution law $\dot{\omega} = \dots$ for variable ω . The details concerning the derivation of the full set of constitutive equations, with no damage, can be found in (Desmorat et al, 2017).

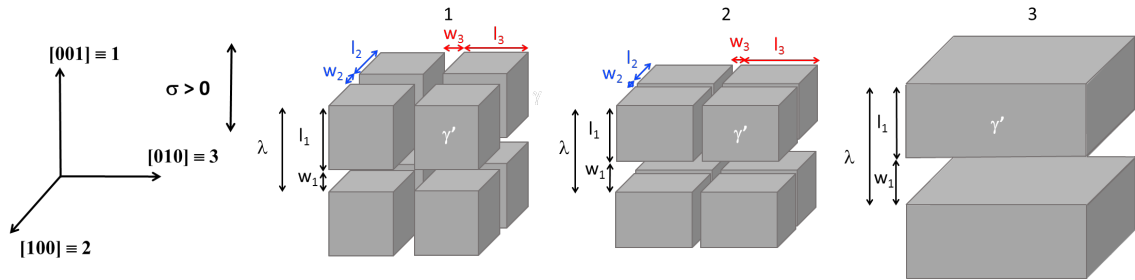


Figure 10: Schematic microstructural evolution in tension creep along the $\langle 001 \rangle$ direction in Natural Anisotropy Basis, reprinted from (Desmorat et al, 2017): 1) initial microstructure ($w_1 = w_2 = w_3 = w_0$), 2) intermediate microstructure ($w_1 > w_2 = w_3$), 3) rafted and coarsened microstructure ($w_1 > w_0, w_2 = w_3 = 0$).

Following Leckie and Onat (1981) and Onat (1984) (working in the context of anisotropic damage by intergranular voids at grain boundaries or by microcracks), Caccuri et al (2018) measure the directional distribution $\Omega(\mathbf{n})$ of the γ channel width for different microstructures degradations. Assuming an expansion of degree q in the components n_i of unit vector \mathbf{n} , $\Omega(\mathbf{n})$ is approximated by an even homogeneous polynomial, $\Omega(\mathbf{n}) = \Omega(-\mathbf{n}) \approx W_{i_1 \dots i_q} n_{i_1} \dots n_{i_q}$, which uniquely defines \mathbf{W} of components $W_{i_1 \dots i_q}$ as a totally symmetric tensor of even order q . A γ channel width tensor of order $q = 2$ corresponds then to a γ channel width directional distribution approximated by

$$\Omega(\mathbf{n}) \approx \mathbf{n} \cdot \mathbf{w} \cdot \mathbf{n} = w_{ij} n_i n_j, \quad \mathbf{w} = \mathbf{w}^T, \quad \|\mathbf{n}\| = 1 \quad (53)$$

which is an homogeneous polynomial of degree 2 in the components n_1, n_2, n_3 of \mathbf{n} and where \mathbf{w} is symmetric γ channel width second order tensor. If needed, the order of the γ channel width tensor can be increased: at order $q = 4$, $\Omega(\mathbf{n}) \approx W_{ijkl} n_i n_j n_k n_l$ with \mathbf{W} totally symmetric, i.e. $W_{ijkl} = W_{jikl} = W_{klij} = W_{ikjl}$, with 15 independent components. Caccuri et al (2018) compare different tensorial orders for \mathbf{W} .

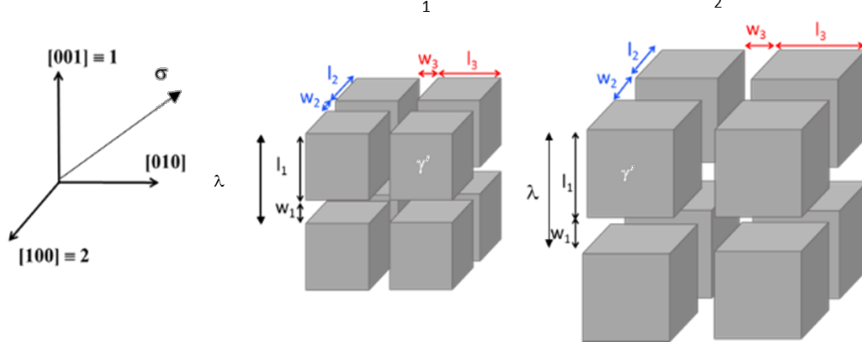


Figure 11: Schematic microstructural evolution in pure coarsening mode (i.e. pure thermal expansion): 1) initial microstructure ($w_1 = w_2 = w_3 = w_0$), 2) final microstructure ($w_1 = w_2 = w_3 > w_0$),

We recall that totally symmetric tensors of order q are isomorphic to homogeneous polynomials of degree q in three variables x_i (or n_i above), $i = 1, 2, 3$, they have $(q + 1)(q + 2)/2$ independent components. Such tensors are —uniquely— defined by polarization (Olive et al, 2017b, Gorodentsev, 2017, p.35) from an homogeneous polynomial of degree q .

7.2. Proposed model (Part I Mechanics)

The first part of constitutive equations for cubic elasto-visco-plasticity coupled with tensorial rafting and damage are:

- elasticity law coupled with damage,

$$\tilde{\sigma} = \frac{\sigma'}{1-D} + \frac{1}{3} \left[\frac{\langle \text{tr } \sigma \rangle_+}{1-D} + \langle \text{tr } \sigma \rangle_- \right] \mathbf{1}, \quad \tilde{\sigma} = \mathbb{E} : (\epsilon - \epsilon^p) \quad (54)$$

with Hooke's tensor \mathbb{E} of cubic symmetry class. It defines the Kelvin projectors \mathbb{P}^d and $\mathbb{P}^{\bar{d}}$ by Eq. (19).

- effective stress partition in cubic symmetry,

$$\tilde{\sigma} = \tilde{\sigma}^d + \tilde{\sigma}^{\bar{d}} + \frac{1}{3} \text{tr } \tilde{\sigma} \mathbf{1} \quad \tilde{\sigma}_{eq}^d = \sqrt{\frac{3}{2} \tilde{\sigma}^d : \tilde{\sigma}^d} \quad \tilde{\sigma}_{eq}^{\bar{d}} = \sqrt{\frac{3}{2} \tilde{\sigma}^{\bar{d}} : \tilde{\sigma}^{\bar{d}}} \quad (55)$$

introducing effective equivalent von Mises norms $\tilde{\sigma}_{eq}^d = \sigma_{eq}^d / (1-D)$ and $\tilde{\sigma}_{eq}^{\bar{d}} = \sigma_{eq}^{\bar{d}} / (1-D)$, with $\tilde{\sigma}^d = \mathbb{P}^d : \tilde{\sigma}$, $\tilde{\sigma}^{\bar{d}} = \mathbb{P}^{\bar{d}} : \tilde{\sigma}$.

- criterion functions with Orowan stress effect: Hill criterion for f_1 , non quadratic norm for f_2 ,

$$f_1 = \tilde{\sigma}_{\text{Hill}} - \frac{\kappa_{\text{ORO}} G}{\|\omega\|} - \sigma_y, \quad f_2 = \|\tilde{\sigma}^{\bar{d}}\|_a - \varpi \frac{\kappa_{\text{ORO}} G}{\|\omega\|} - \bar{\sigma}_y \quad (56)$$

where

$$\tilde{\sigma}_{\text{Hill}} = \sqrt{\frac{3}{2} (\tilde{\sigma}^d : \tilde{\sigma}^d + h^2 \tilde{\sigma}^{\bar{d}} : \tilde{\sigma}^{\bar{d}})}, \quad \|\tilde{\sigma}^{\bar{d}}\|_a = 3 \left(\frac{1}{6} \sum_{i \neq j} |\tilde{\sigma}_{ij}^{\bar{d}}|^a \right)^{\frac{1}{a}} \quad (57)$$

- accumulated plastic strain rates,

$$\dot{p}_1^{\text{Hill}} = \sqrt{\frac{2}{3} \left(\dot{\epsilon}_1^{pd} : \dot{\epsilon}_1^{pd} + \frac{1}{h^2} \dot{\epsilon}_1^{p\bar{d}} : \dot{\epsilon}_1^{p\bar{d}} \right)}, \quad \dot{p}_2^{\bar{d}} = 2 \left(\frac{1}{6} \sum_{i \neq j} |\dot{\epsilon}_{ij}^p|^{\frac{a}{a-1}} \right)^{\frac{a-1}{a}} \quad (58)$$

- normality rule and normal \mathbf{n}^d ,

$$\dot{\epsilon}^p = \dot{p}_1^{\text{Hill}} \frac{\partial f_1}{\partial \tilde{\sigma}} + \dot{p}_2^{\bar{d}} \frac{\partial f_2}{\partial \tilde{\sigma}}, \quad \mathbf{n}^d = \left(\frac{\partial f_1}{\partial \tilde{\sigma}} \right)^d = \mathbb{P}^d : \frac{\partial f_1}{\partial \tilde{\sigma}} \quad (59)$$

Comparison with Eq. (41) shows that $\dot{r}_1 = (1-D)\dot{p}_1^{\text{Hill}}$, $\dot{r}_2 = (1-D)\dot{p}_2^{\bar{d}}$.

- viscosity laws, formulated in a different manner for f_1 and for f_2 criteria to represent well the high strain rate viscosity,

$$\dot{p}_1^{\text{Hill}} = \left\langle -\frac{\sigma_{\text{v}\infty}}{K_N} \ln \left(1 - \frac{f_1}{\sigma_{\text{v}\infty}} \right) \right\rangle^N, \quad \dot{p}_2^{\text{d}} = \left\langle \frac{f_2}{\bar{K}_N} \right\rangle^{\bar{N}} \frac{1}{\max(\bar{\kappa}(\|\bar{\sigma}^{\text{d}}\|_a - \bar{\sigma}_0), 1)} \quad (60)$$

The material parameters are: E , ν , G for elasticity, yield stresses σ_y and $\bar{\sigma}_y$, Hill's parameter h and parameter a for non quadratic norm, parameters κ_{ORO} and ϖ for Orowan stress effect, Norton's viscosity parameters K_N , N , \bar{K}_N , \bar{N} and high strain rate viscosity parameters $\sigma_{\text{v}\infty}$ and $\bar{\kappa}$, $\bar{\sigma}_0 = \sigma_{\text{lim}}^\mu$.

Parameter a has an important effect in torsion as illustrated by the Finite Element computation of Appendix B. It has no effect at all for an uniaxial loading along $\langle 001 \rangle$ nor for an uniaxial loading along $\langle 111 \rangle$.

7.3. Proposed model (Part II Microstructure degradation)

The second part of constitutive equations concerns the microstructure degradation occurring at high temperature and the evolution law for the γ channel width variables ω and \mathbf{w} .

- evolution law for dimensionless γ channel width variable ω ,

$$\dot{\omega} = \dot{\omega}^{\text{raft}} + \dot{\omega}_{\text{mc}} \mathbf{1} + \sqrt{3} \dot{\omega}_{\text{LSW}} \frac{\omega}{\|\omega\|} \quad (61)$$

where rafting contribution (through tensor ω^{raft}), mechanical coarsening contribution (through isotropic contribution ω_{mc}) and homothetic growth contribution (diffusion controlled isotropic coarsening of γ' particles in the absence of applied stress (Lifshitz and Slyozov, 1961, Wagner, 1961) satisfy

$$\begin{cases} \dot{\omega}^{\text{raft}} = K_{\text{raft}} \exp(u_{\text{raft}} \min(\bar{\sigma}_{\text{eq}}^{\text{d}}, \sigma_{\text{lim}}^\mu)) \mathcal{H}(p_1^{\text{Hill}} - \varepsilon_{\text{th}}^p) \mathcal{H} \mathbf{n}^{\text{d}} \\ \dot{\omega}_{\text{mc}} = K_{\text{mc}} \exp(u_{\text{mc}} \bar{\sigma}_{\text{eq}}^{\text{d}}) \mathcal{H}(p_2^{\text{d}} - \bar{\varepsilon}_{\text{th}}^p) \\ \dot{\omega}_{\text{LSW}} = \frac{K_{\text{LSW}}}{3\omega_{\text{LSW}}^2} \end{cases} \quad (62)$$

with $\mathcal{H} = \mathcal{H}(\mathcal{D}) = 0$ or 1 , Heaviside function of the intrinsic dissipation.

The initial values are: $\omega_{\text{LSW}}(t=0) = 1$, $\omega^{\text{raft}}(t=0) = \mathbf{0}$, $\omega_{\text{mc}}(t=0) = 0$ and $\omega(t=0) = \mathbf{1}$. See Appendix C for the stress triaxiality effect.

- γ channel width tensor,

$$\mathbf{w} = w_0 \omega \quad (63)$$

gained from initial temperature dependent value w_0 ($w_0 = 80\text{nm}$ for CMSX-4 at 1050°C),

- minimum eigenvalues ω_i (resp. w_i) of second order tensor ω (resp. \mathbf{w}) bounded to zero.

Note that a particular Heaviside function \mathcal{H} (of values 0 or 1) is introduced in evolution law (62), with most often $\mathcal{H} = 1$. As described in (Desmorat et al, 2017) the value $\mathcal{H} = 0$ is set only when needed to enforce an always positive intrinsic dissipation (see Section 7.5).

The material parameters for microstructure evolution are w_0 , K_{raft} , u_{raft} , σ_{lim}^μ , $\varepsilon_{\text{th}}^p$, K_{mc} , $\bar{\varepsilon}_{\text{th}}^p$ and K_{LSW} . The visco-plasticity normal \mathbf{n}^{d} is a deviatoric second order tensor introduced by Tinga et al (2009a), it is defined Eq. (59). Second order tensor $\omega^{\text{raft}} = (\omega^{\text{raft}})'$ is deviatoric.

7.4. Proposed model (Part III Damage)

The constitutive equations for final (damage) part of the model are those derived in Sections 6.1 and 6.2 with $A_{\text{dis}} = 0$. They are recalled here.

- Rate dependent threshold criterion,

$$f_D = \hat{P} - 1 \quad (64)$$

such as $f_D < 0 \rightarrow$ no damage, $f_D \geq 0 \rightarrow$ damage growth, with

$$\hat{P} = \sup_i \left[\frac{p^{\text{d}}}{\varepsilon_{pD}^0} \exp\left(-B\left\langle 1 - \frac{\dot{p}_0}{\dot{p}^{\text{d}}}\right\rangle\right) + \frac{p^{\text{d}}}{\bar{\varepsilon}_{pD}^0} \exp\left(-\bar{B}\left\langle 1 - \frac{\dot{p}_0}{\dot{p}^{\text{d}}}\right\rangle\right) \right] \quad (65)$$

- Damage evolution law,

$$\dot{D} = R_v \left(A \dot{p}^d + \bar{A} \dot{p}^{\bar{d}} \right) H(f_D) \quad (66)$$

where triaxiality function

$$R_v = \frac{2}{3}(1 + \nu) \left(\frac{\tilde{\sigma}_{eq}^d}{\tilde{\sigma}_{HIII}^d} \right)^2 + \frac{E}{3G} \left(\frac{\tilde{\sigma}_{eq}^{\bar{d}}}{\tilde{\sigma}_{HIII}^{\bar{d}}} \right)^2 + 3(1 - 2\nu) \left\langle \frac{\tilde{\sigma}_H}{\tilde{\sigma}_{HIII}^+} \right\rangle^2 \quad (67)$$

is equivalent to definition (35) due to damage isotropy.

Failure by crack initiation occurs when the damage D reaches the critical value D_c (measured equal to $D_c = 0.15$ from all $\langle 001 \rangle$ and $\langle 111 \rangle$ creep and tension tests). Material parameters ϵ_{pD}^0 and $\bar{\epsilon}_{pD}^0$ are the damage thresholds in creep, respectively measured in $\langle 001 \rangle$ and in $\langle 111 \rangle$ creep, \dot{p}_0 , $\dot{\bar{p}}_0$, B , \bar{B} are the rate dependency parameters, A , \bar{A} are the damage parameters.

7.5. Positivity of the intrinsic dissipation

We consider the thermodynamics framework for microstructural changes, including rafting, of Desmorat et al (2017) for CMSX-4 within Lemaitre (1992) damage framework.

Helmholtz free energy density becomes function of the internal variables $r_1 \geq 0$ and $r_2 \geq 0$ homogeneous to accumulated plastic strains for isotropic hardening (whose effect on the yield stress is not modeled here) and of tensorial mechanical rafting variable $\omega = \mathbf{w}/w_0(f_{\gamma'}(T))$,

$$\rho\psi = \rho\psi_e + \frac{\kappa_{ORO}G}{\|\omega\|} (r_1 + \varpi r_2) + \frac{1}{2} (\kappa_u - \kappa_\omega \omega_{eq}) \delta_u^2 \quad (68)$$

where $\rho\psi_e = \frac{1}{2}(\epsilon - \epsilon^p) : \mathbb{E}(1 - D) : (\epsilon - \epsilon^p)$ is the Legendre transform of potential (4.5) and where $\omega_{eq} = \sqrt{\frac{3}{2}}\|\omega'\|$ is von Mises norm of symmetric second order tensor ω ; κ_u , κ_ω and the misfit δ_u are material parameters (Fedelich et al, 2009). For the sake of simplicity the thermal expansion and heat capacity contributions have been omitted.

The criterion functions are those defined Eq. (56), function of Orowan stress $\sigma_{ORO} = \kappa_{ORO}G/\|\omega\|$. Due to the use of non quadratic norm for f_2 and $\dot{p}_2^{\bar{d}}$ (given by (58)), the dissipation $\sigma : \dot{\epsilon}^p + Y\dot{D}$ due to visco-plasticity and damage (42) writes

$$\mathcal{D}_1 = (1 - D) \left(\tilde{\sigma}_{HIII} \dot{p}_1^{HIII} + \|\tilde{\sigma}^{\bar{d}}\|_a \dot{p}_2^{\bar{d}} \right) + Y\dot{D} \geq 0 \quad (69)$$

Recall that $(1 - D) \dot{p}_1^{HIII} = \dot{r}_1 \geq 0$ and $(1 - D) \dot{p}_2^{\bar{d}} = \dot{r}_2 \geq 0$. As $Y \geq 0$ and $D \leq D_c < 1$, \mathcal{D}_1 is positive.

To the visco-plastic dissipation \mathcal{D}_1 is added the dissipation \mathcal{D}_2 due to microstructure degradation, by rafting, mechanical coarsening and homothetic growth,

$$\mathcal{D}_2 = \mathbf{\Omega} : \dot{\omega} \quad (70)$$

with

$$\mathbf{\Omega} = -\rho \frac{\partial \psi}{\partial \omega} = \frac{\kappa_{ORO}G}{\|\omega\|^2} \frac{\omega}{\|\omega\|} (r_1 + \varpi r_2) + \sqrt{\frac{3}{8}} \kappa_\omega \delta_u^2 \frac{\omega'}{\|\omega'\|} \quad (71)$$

the thermodynamics force associated with the internal variable ω .

The evolution law (61), coupled with damage by means of the effective stress in the scalar prefactors of (62), is of generic form

$$\dot{\omega} = \dot{\mathcal{R}} \mathcal{H} \mathbf{n}^d + \dot{C} \mathbf{1} + \dot{\mathcal{G}} \frac{\omega}{\|\omega\|} \quad (72)$$

with normal \mathbf{n}^d defined by Eq. (59) and where $\dot{\mathcal{R}} \geq 0$ (for rafting phenomenon), $\dot{C} \geq 0$ (for mechanical coarsening), $\dot{\mathcal{G}} \geq 0$ (for homothetic growth). Under these conditions completed with

$$\mathcal{H} = H(\mathcal{D}) \quad i.e. \quad \begin{cases} \mathcal{H} = 1 & \text{if } \mathcal{D} \geq 0, \\ \mathcal{H} = 0 & \text{if } \mathcal{D} < 0 \end{cases} \quad (73)$$

it is proved in (Desmorat et al, 2017) that $\mathcal{D}_2 \geq 0$.

The total intrinsic dissipation

$$\mathcal{D} = \mathcal{D}_1 + \mathcal{D}_2 \geq 0 \quad (74)$$

is therefore positive for any loading, isothermal or not, proportional or not. The second principle of thermodynamics is fulfilled by proposed constitutive equations coupled with damage.

8. Creep and monotonic failure of cubic CMSX-4 superalloy at 1050°C

Let us finally present the responses of the proposed set of constitutive equations (parts I, II and III) coupling microstructural changes, visco-plasticity and mechanical damage. Rupture corresponds to $D = D_c = 0.15$, the damage value at which are stopped the computations, whatever the loading type or direction.

8.1. Computed stress-strain curves

The true stress-true strain tension curves are plotted in Fig. 12. The increase of ductility with the strain rate is well obtained, due to proposed rate dependent damage threshold (the plateaux or the gradual (linear) softening are at zero damage). It is here recalled that there is no isotropic (nor kinematic) hardening in the modeling (parameters $R_\infty = \bar{R}_\infty = 0$) so that one can expect a better fit of the pre-plateau curves for $\langle 111 \rangle$ orientation if introduced. Also, the modeling of the initial (quick) softening at strains lower than 0.03 is left to further work (note that this usually requires a multi scale modeling (Tinga et al, 2009a, Kindrachuk and Fedelich, 2012)).

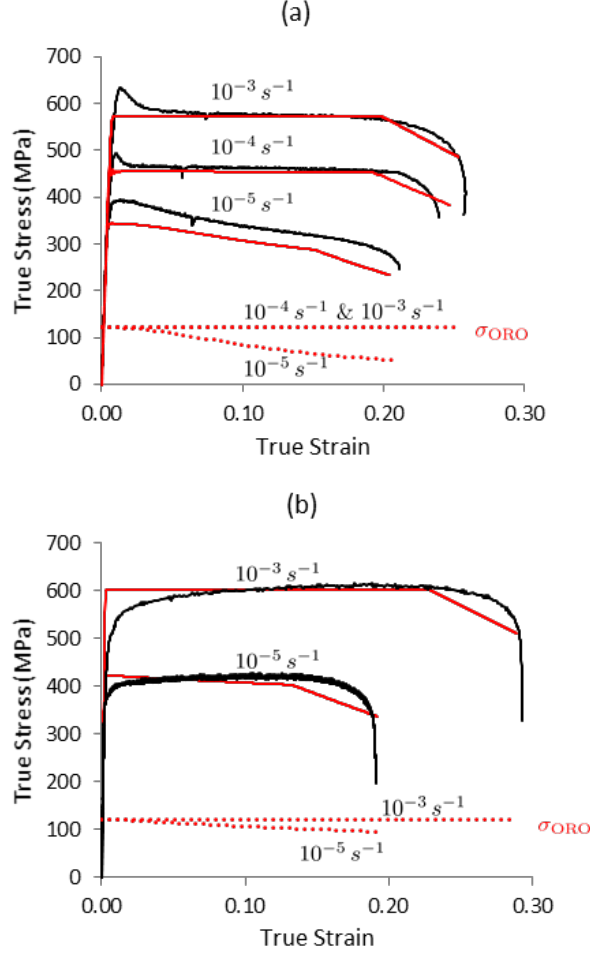


Figure 12: Full model response for $\langle 001 \rangle$ and $\langle 111 \rangle$ tension curves at different strain rates (CMSX-4 at 1050°C). Computed Orowan stress σ_{ORO} reported.

8.2. Computed microstructure degradation in creep

The microstructure evolution of the different specimens tested in creep is plotted in Fig. 13 and compared to experiments with a good agreement. The w_i are the 3 principal components of the γ channel width tensor, here in Natural Anisotropy Basis, either measured (bullets) or computed (lines).

- For $\langle 001 \rangle$ orientation: longitudinal mean channel width w_1 measured in the loading direction increases when the transverse widths $w_2 = w_3 \rightarrow 0$. This is a macroscopic representation of the phenomenon of rafting. The effect of the stress level is well obtained for creep in $\langle 001 \rangle$ orientation, enhanced by the damage at plastic strain larger than 0.05.
- For $\langle 111 \rangle$ orientation: the 3 components remain equal $w_1 = w_2 = w_3$ and increase with time. This is the representation of the phenomenon of mechanical coarsening, here stress independent.

Note that under loading the LSW homothetic growth term ω_{LSW} (Eq. (61)) has a negligible contribution. The effect of damage on the microstructural changes is quite small.

8.3. Computed creep curves

The creep responses are given in Fig. 14, also with a very good agreement. We have made the choice of a critical damage independent from the loading direction, therefore identical for $\langle 001 \rangle$ creep and for $\langle 111 \rangle$ creep. This is why the creep curves for $\langle 111 \rangle$ crystallographic orientation look shorter than the experimental ones. The time to failure is nevertheless very accurate for both orientations.

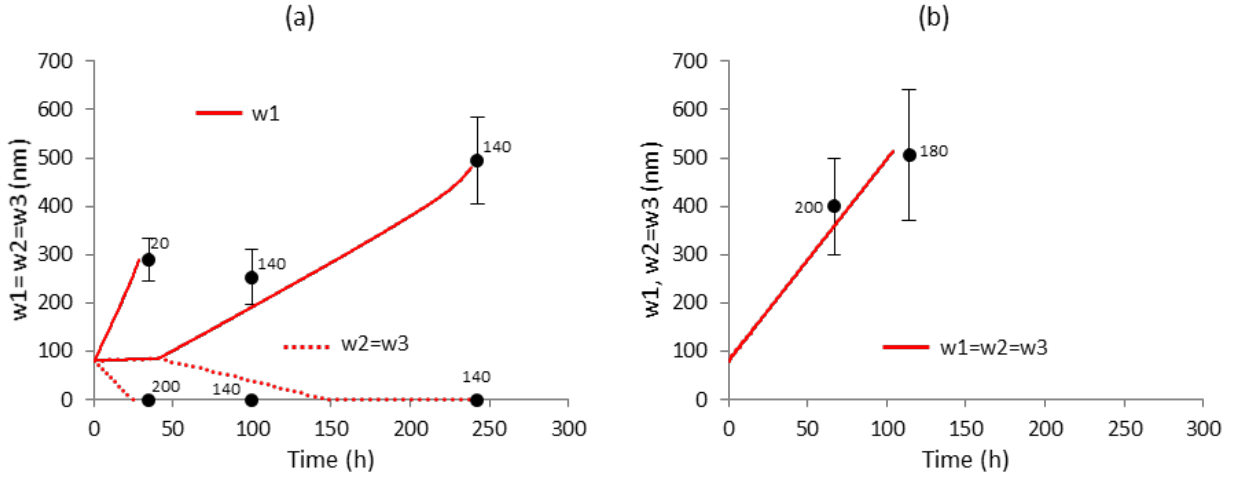


Figure 13: Evolution of the microstructure in creep of CMSX-4 at 1050°C: (a) $\langle 001 \rangle$ creep, applied stress levels: $\sigma = 140$ MPa, $\sigma = 200$ MPa, (b) $\langle 111 \rangle$ creep, stress levels: $\sigma = 180$ MPa, $\sigma = 200$ MPa (bullets: observations, solid lines: model).

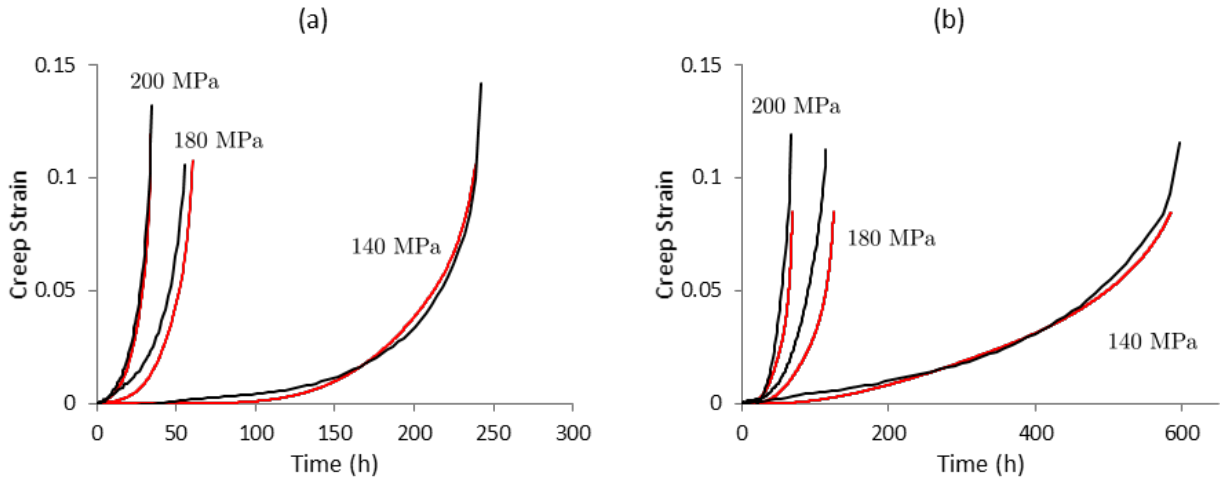


Figure 14: Full model response for $\langle 001 \rangle$ and $\langle 111 \rangle$ creep at different stress levels (CMSX-4 at 1050°C, $\sigma = 140, 180, 200$ MPa).

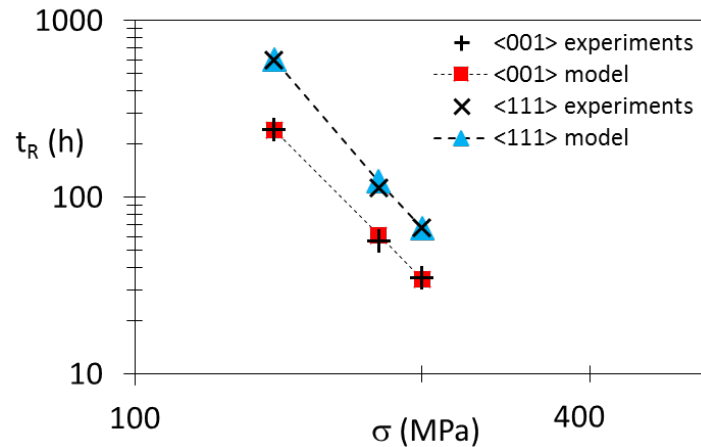


Figure 15: Comparison between the creep lifetimes measured after experimental tests along $\langle 001 \rangle$ and along $\langle 111 \rangle$ and the ones predicted by the model at $D = D_c = 0.15$.

9. Remarks on proposed modeling in the limiting case of isotropic visco-plasticity

If one assumes Hill's parameter $h = 1$, the criterion f_1 becomes isotropic von Mises criterion. If furthermore $\bar{\sigma}_y \rightarrow \infty$, the second viscosity is deactivated as $\epsilon_2^p = 0$ (with then $\epsilon^p = \epsilon_1^p$ and $p_1^{\text{Hill}} = p$). Previous visco-plasticity

coupled with damage constitutive equations become isotropic.

A few comments can then be made.

- The viscosity law (60) recovers Norton's law $\sigma_v \approx K_N \dot{p}^{1/N}$ at low strain rates, with $f_1 = \sigma_v$ equal to the viscous stress when yielding. Remark also that the viscosity law is inverted into

$$\sigma_v = \sigma_{v\infty} \left(1 - \exp \left(- \frac{K_N}{\sigma_{v\infty}} \dot{p}^{1/N} \right) \right) \quad (75)$$

a form which exhibits the saturation of the viscous stress σ_v (to $\sigma_{v\infty}$) at high strain rate.

- An isotropic rate dependent damage threshold criterion f_D , such as $f_D < 0 \rightarrow$ no damage growth, $f_D \geq 0 \rightarrow$ damage growth, is obtained as

$$f_D = \hat{P} - 1, \quad \hat{P} = \sup_t \left[\frac{p}{\epsilon_{pD}^0} \exp \left(- B \left(1 - \frac{\dot{p}_0}{\dot{p}} \right) \right) \right] \quad (76)$$

- In creep (at low strain rate) one has $1 - \frac{\dot{p}_0}{\dot{p}} < 0$ so that $\hat{P} \approx p / \epsilon_{pD}^0$ and one recovers standard constant threshold of Lemaitre (1992), $p < p_D = \epsilon_{pD}^0 \rightarrow$ no damage growth.
- The material parameter B is related to both the damage threshold in creep (at low strain rate) ϵ_{pD}^0 and the damage threshold in tension at infinite strain rate ϵ_{pD}^∞ as

$$B = \ln \left(\frac{\epsilon_{pD}^\infty}{\epsilon_{pD}^0} \right) \quad (77)$$

At high strain rate $1 - \frac{\dot{p}_0}{\dot{p}} \approx 1$, one has then $\hat{P} \approx p e^{-B} / \epsilon_{pD}^0$ so that the damage threshold becomes

$$p < p_D = \epsilon_{pD}^0 e^B = \epsilon_{pD}^\infty \rightarrow \text{no damage growth.} \quad (78)$$

- There is no Lode angle dependency in the damage modeling obtained in this limiting case, as there is none in initial Lemaitre's damage law for isotropic materials. To model this dependency in Lemaitre and Chaboche (1985,1991) damage framework consider the works of Malcher and Mamiya (2014) and of Cao et al (2014) or, as discussed in (Desmorat, 2012, 2015), consider anisotropic damage (which always introduce a Lode angle dependency of the damage growth).

10. Conclusion

A phenomenological damage model has been proposed to describe the (anisotropic) strain rate sensitivity of damage onset and evolution in single crystal superalloys. A novel strain rate sensitive damage threshold has been introduced, which allows to describe the damage onset dependence on the strain rate during creep and monotonic tension. A novel formulation of the Kelvin projectors is proposed for cubic material symmetry as well. This latter, based on the harmonic decomposition of the elasticity tensor, allows to determine the Kelvin projectors for cubic material symmetry without solving any eigenvalues problem.

The curves obtained for the CMSX-4 at 1050°C along the $\langle 001 \rangle$ and $\langle 111 \rangle$ crystallographic directions show that, thanks to this model, tertiary creep, time to rupture and ductility can be quite accurately described for single crystal superalloys. However, the proposed damage can be extended to other materials, possibly isotropic or of other material symmetry class, deforming and degrading by mechanisms different from the ones observed in single crystal superalloys but still exhibiting a rate dependent ductility.

Recall that no hardening, neither isotropic nor kinematic, has been introduced. This was not necessary for considered monotonic applications at 1050°C, but hardening and primary creep is observed at other temperatures for CMSX-4 (Svoboda and Lukas, 1998, Matan et al, 1999a, Reed et al, 1999, Epishin et al, 2001, Jun Chang et al, 2018). Further modeling effort must focus on kinematic hardening: indeed it has been shown by Sermage (1998), Sermage et al (2000), but for isotropic steels, that kinematic hardening plays a major role in the nonlinearity of the creep-fatigue interaction. Power laws for kinematic hardening may also prove useful (Desmorat, 2010, 2013). The generalization to cubic symmetry of existing hardening rules and associated constitutive equations for primary creep is left to further work.

Acknowledgements

The authors are grateful to Safran Helicopter Engines for funding this work. C. Moriconi, A. Burtreau and Z. Hervier (all three at Safran Helicopter Engines) are especially thanked for their continuous interest in this study, T. Rose (SafranTech) is acknowledged for the numerical implementation in ZSet computer code.

A. Harmonic decomposition of cubic elasticity tensor in its Natural Anisotropy Basis

In Natural Anisotropy Basis (NAB) the generalized Lamé constants of harmonic decomposition are, using Eq. (9),

$$\lambda = \frac{1}{5}(E_{1111} - 2E_{1212} + 4E_{1122}) = \frac{1}{5} \left(\frac{1 + 3\nu}{1 - \nu - 2\nu^2} E - 2G \right) \quad (79)$$

$$\mu = \frac{1}{5}(E_{1111} + 3E_{1212} - E_{1122}) = \frac{1}{5} \left(\frac{E}{1 + \nu} + 3G \right) \quad (80)$$

The harmonic fourth order part \mathbb{H} carries both the third cubic elasticity parameter and the Natural Anisotropy Basis (NAB) of cubic symmetry. It has for Kelvin matrix representation, in Natural Anisotropy Basis still (Auffray et al, 2014)

$$[\mathbb{H}] = \delta \begin{bmatrix} 8 & -4 & -4 & 0 & 0 & 0 \\ -4 & 8 & -4 & 0 & 0 & 0 \\ -4 & -4 & 8 & 0 & 0 & 0 \\ 0 & 0 & 0 & -8 & 0 & 0 \\ 0 & 0 & 0 & 0 & -8 & 0 \\ 0 & 0 & 0 & 0 & 0 & -8 \end{bmatrix}_{NAB} \quad (81)$$

with invariant δ defined by Eq. (14). In terms of components:

$$\delta = \frac{1}{20}(E_{1111} - 2E_{1212} - E_{1122}) = \frac{1}{4}(\mu - G) \quad (82)$$

The condition $\mathbb{H} = \mathbf{0}$ corresponds to $\delta = 0$ and to $\mu = \frac{E}{2(1+\nu)} = G$, *i.e.* to isotropic elasticity. And keep in mind that E, ν, G but also λ, μ, δ and $\mu - G = 4\delta$ are (non independent) invariants of cubic elasticity tensor \mathbb{E} .

B. Consequences on torsion of non quadratic norm in criterion function f_2

A non quadratic norm is used within second criterion function f_2 . This is a key-point allowing to represent the feature of several yield zones observed in torsion of single crystals such as CMSX-4.

Remark first that the uniaxial model response for applied stresses in orientation $\langle 001 \rangle$ and in orientation $\langle 111 \rangle$ remains for any value of parameter a the same as the one of simpler (quadratic) case $a = 2$, which corresponds to $\|\tilde{\sigma}^d\|_2 = \tilde{\sigma}_{eq}^d$.

In torsion around axis $y \equiv 2 \equiv [010]$, a value $a \in]1, 2[$ allows to model a non homogeneous plastic strain field (Fig. 16), as observed experimentally by Nouailhas and Cailletaud (1995). The prescribed rotation for the Finite Element computation is such that the damage D remains equal to zero at all points.

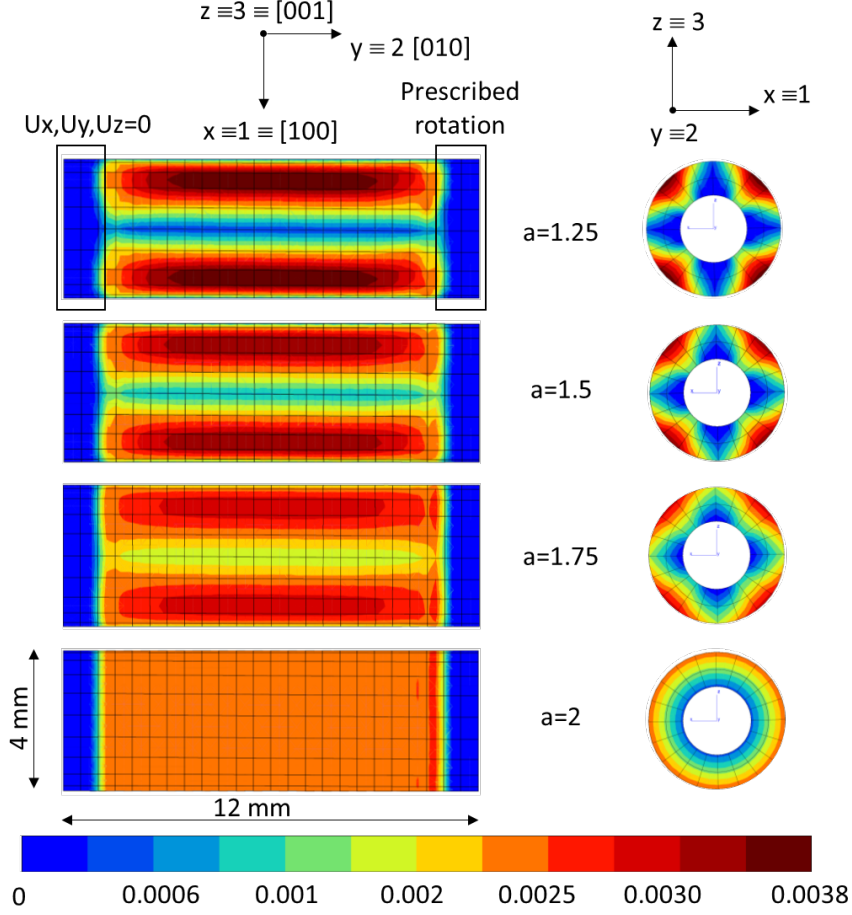


Figure 16: Map of equivalent plastic strain field $\sqrt{\frac{2}{3}}\|\epsilon^p(\mathbf{x})\|$ in torsion. Geometry = tube of length 12 mm, of diameter 4 mm, of thickness 1 mm. Left and right nodes rigidly linked, prescribed rotation $\alpha = 2$ rad around [010]-axis.

C. Triaxiality effect on microstructure evolution

The stress triaxiality has an effect on the microstructure evolution, compressive loads inducing slower evolutions than positive ones. A way to model this is to replace the (effective) von Mises equivalent stress $\tilde{\sigma}_{eq}^d = (\tilde{\sigma}^d)_{eq}$ in evolution law (62) by a Drucker-Prager stress, *i.e.* by setting

$$\begin{cases} \dot{\omega}^{\text{raft}} = K_{\text{raft}} \exp\left(u_{\text{raft}} \min(\tilde{\sigma}_{\text{DP}}^d, \sigma_{\text{lim}}^\mu)\right) H(p_1^{\text{Hill}} - \varepsilon_{\text{th}}^p) \mathcal{H} \mathbf{n}^d \\ \dot{\omega}_{\text{mc}} = K_{\text{mc}} \exp\left(u_{\text{mc}} \min(\tilde{\sigma}_{\text{DP}}^d, \sigma_{\text{lim}}^\mu)\right) H(p_2^d - \bar{\varepsilon}_{\text{th}}^p) \\ \dot{\omega}_{\text{LSW}} = \frac{K_{\text{LSW}}}{3\omega_{\text{LSW}}^2} \end{cases} \quad (83)$$

where

$$\tilde{\sigma}_{\text{DP}}^d = \zeta \tilde{\sigma}_{eq}^d + (1 - \zeta) \text{tr} \tilde{\sigma} \quad (84)$$

and

$$\tilde{\sigma}_{\text{DP}}^{\bar{d}} = \zeta \tilde{\sigma}_{eq}^{\bar{d}} + (1 - \zeta) \text{tr} \tilde{\sigma} \quad (85)$$

with ζ a material parameter (possibly different in each definition).

D. Material parameters

The initial yield stresses are zero, $\sigma_y = \bar{\sigma}_y = 0$ and there is no hardening introduced at 1050°C.

The material parameters for the microstructure change and damage identified at this temperature are:

- the elasticity parameters, $E = 88000$ MPa, $\nu = 0.4$, $G = 96150$ MPa,
- the initial γ channel width $w_0 = 80$ nm and γ' volume fraction $f_{\gamma'} = 0.54$;

- $\kappa_{\text{ORO}} = 2.2 \cdot 10^{-3} \text{ MPa}^{-1}$, $\varpi = 0.85$ for the Orowan stress effect;
- $K_{\text{LSW}} = 1.1 \cdot 10^{-6} \text{ s}^{-1}$ for LSW homothetic growth;
- $\varepsilon_{\text{th}}^p = 5 \cdot 10^{-5}$ and $\bar{\varepsilon}_{\text{th}}^p = 0^+$ for Matan *et al* thresholds in terms of plastic strain;
- $K_{\text{raft}} = 2.2 \cdot 10^{-7} \text{ s}^{-1}$, $u_{\text{raft}} = 0.0233$, $\sigma_{\text{lim}}^{\mu} = 280 \text{ MPa}$ for rafting;
- $K_{\text{mc}} = 1.4 \cdot 10^{-5} \text{ s}^{-1}$, $u_{\text{mc}} = 0.0012$, for mechanical coarsening;
- the damage thresholds in creep $\varepsilon_{pD}^0 = 0.05$ and $\bar{\varepsilon}_{pD}^0 = 0.025$;
- $\dot{p}_0 = 2 \cdot 10^{-6} \text{ s}^{-1}$, $\ddot{p}_0 = 2.5 \cdot 10^{-6} \text{ s}^{-1}$, $B = 1.35$, $\bar{B} = 2.21$, for the rate dependency of the damage threshold;
- $A = 2.8$, $\bar{A} R_{\gamma}^{(111)} = 2.5$ as damage parameters;
- the critical damage $D_c = 0.15$ (take $D_c = 0.999$ for Finite Elements computations).

References

- Altenbach H., Kruch S., 2013, Advanced Materials Modelling for Structures, Vol 19 of Advanced Structured Materials Series, Springer, ISBN 978-3-642-35166-2.
- Arramon, Y.P., Mehrabadi, M.M., Martin, D.W., Cowin, S.C., 2000. A multidimensional anisotropic strength criterion based on Kelvin modes. *Int. J. Solids Struct.* 37, 2915–2935.
- Asaro, R., 1983. Crystal Plasticity. *J. Appl. Mech. ASME*, 50, 921–934.
- Asaro, R., Lubarda, V., 2006. *Mechanics of Solids and Materials*. Cambridge University Press.
- Aslan O., Cordero N.M., Gaubert A., Forest S., 2011, Micromorphic approach to single crystal plasticity and damage, *International Journal of Engineering Science*, 49, 1311–1325.
- Auffray N., Kolev B., Petitot M., 2014. On anisotropic polynomial relations for the elasticity tensor. *J. of Elasticity*, 115(1), 77–103.
- Backus G., 1970. A geometrical picture of anisotropic elastic tensors, *Rev. Geophys.*, 8(3):633–671.
- Baerheim R., 1993. Harmonic decomposition of the anisotropic elasticity tensor, *Quarterly Journal of Mechanics and Applied Mathematics A.*, 46, 3, 391–41.
- Benallal, A., Billardon, R., Doghri, I., An integration algorithm and the corresponding consistent tangent operator for fully coupled elastoplastic and damage equations, *Comm. Appl. Numer. Meth.*, 4, 731–740, 1988.
- Benyoucef, M. Clement, N., Coujou, A., 1993. Transmission electron microscopy in situ deformation of MC2 superalloy at room temperature. *Mater. Sci. Eng. A164*, 401–406.
- Bertram, A., Olschewski, J., 1996. Anisotropic creep modelling of the single crystal superalloy SRR99. *Comp. Mater. Sci.* 5, 12–16.
- Besseling J.F., van der Giessen E., 1994, *Mathematical Modelling of Inelastic Deformation*, London, Chapman & Hall.
- Besson J., Damage of ductile materials deforming under multiple plastic or viscoplastic mechanism, *International Journal of Plasticity* 25, 2204–2221, 2009.
- Besson J., 2009, Continuum Models of Ductile Fracture: A Review, *International Journal of Damage Mechanics* 19(1), pp. 3–52.
- Biegler, M.W., Mehrabadi, M.M., 1995. An energy-based constitutive model for anisotropic solids subject to damage. *Mech. Mater.* 19, 151–164.
- Biermann, H., Grossman, B.V., Schneider, T., Feng, H., Mughrabi, H., 1996. Investigation of the γ/γ' morphology and internal stresses in a monocrystalline turbine blade after service: determination of the local thermal and mechanical loads. R.D. Kissinger, D.J. Deye, D.L. Anton, A.D. Cetel, M.V. Nathal, T.M. Pollock, D.A. Woodford (Eds.) *Superalloys 1996*, TMS, Seven Springs, Champion, PA, USA, 201–210.
- Boehler J.-P., Kirillov A. A., Jr., Onat E. T., 1994, On the polynomial invariants of the elasticity tensor, *J. Elasticity*, 34(2):97–110.
- Borvik T., Hopperstad O.S., Berstad T., Langseth M., Perforation of 12 mm thick steel plates by 20 mm diameter projectiles with flat, hemispherical and conical noses Part II: numerical simulations, *International Journal of Impact Engineering* 27, 37–64, 2002.
- Bouchard P.O., Bourgeon L., Fayolle S., Mocellin K., 2011, An enhanced Lemaitre model formulation for materials processing damage computation, *Int J Mater Form*, 4, 299–315.
- Caccuri V., Desmorat R., Cormier J., Tensorial nature of γ' -rafting evolution in nickel-based single crystal superalloys, *Acta Materialia*, 158, 138–154, 2018.
- Cao T.-S., Gachet J.-M., Montmitonnet P., Bouchard P.-O., 2014, A Lode-dependent enhanced Lemaitre model for ductile fracture prediction at low stress triaxiality, *Engineering Fracture Mechanics*, 80–96.
- Caron, P., Khan, T., 1983. Improvement of creep strength in a nickel-base single crystal superalloy by heat treatment. *Mater. Sci. Eng.* 61, 173–194.
- Caron, P., Ramusat, C., Diologent, F., 2008. Influence of the γ' fraction on the topological inversion during high temperature creep of single crystal superalloys. R. Reed, K. Green, P. Caron, T. Gabb, M. Fahrman, E. Huron, S. Woodard (Eds.) *Superalloys 2008*, TMS, Seven Springs, Champion, PA, USA, 159–167.
- Chaboche J.-L., 1979, Le concept de contrainte effective appliqué à l'élasticité et à la viscoplasticité en présence d'un endommagement anisotrope. In *Col. Euromech 115*, Grenoble, Eds du CNRS 1982.
- Chaboche J.-L., Gaubert A., Kanouté P., Longuet A., Azzouz F., Mazzière M., 2013, Viscoplastic constitutive equations of combustion chamber materials including cyclic hardening and dynamic strain aging, *International Journal of Plasticity*, 46, 1–22.
- Chu C.C., Needleman A., Void nucleation effects in biaxially stretched sheets, *J. Eng. Mater. Technol.* 102, 249–256, 1980.
- Cormier J., 2006. *Comportement en fluage isotherme à haute et très haute température du superalliage monocristallin MC2*, Ph.D. Thesis, ENSMA-Université de Poitiers (France).
- Cormier, J., Cailletaud, G., 2010. Constitutive modeling of the creep behavior of single crystal superalloys under non-isothermal conditions inducing phase transformations. *Mater. Sci. Eng. A527*, 6300–6312.
- Cornet C., Zhao L.G., Tong J., 2011, A study of cyclic behaviour of a nickel-based superalloy at elevated temperature using a viscoplastic-damage model *International Journal of Fatigue* 33, 241–249.
- Cowin S. C., Mehrabadi M.M., Eigentensors of linear anisotropic elastic materials, *Q. J. Mech. Appl. Math.*, 43, 15–41, 1990.
- Cowin, S., Mehrabadi, M., Sadegh, A., 1991. Kelvin's Formulation of the Anisotropic Hooke's Law. *SIAM Journal*, J. Wu, T. Ting, and D. Barnett, Soc. Ind. and Applied Math, 340–356.
- Desmorat R., Otin S., Cross-identification isotropic/anisotropic damage and application to anisothermal structural failure, *Engineering Fracture Mechanics*, 75(11), p. 3446–3463, 2008.
- Desmorat R., 2010, Non-saturating nonlinear kinematic hardening laws. *C.R. Mécanique* 338, 146–151.
- Desmorat, R., Marull, R., 2011. Non-quadratic Kelvin modes based plasticity criteria for anisotropic materials. *Int. J. Plasticity* 27, 328–351.

- Desmorat R., Continuum approach in damage mechanics. In: Summer school hardening and damage of materials under finite deformations, constitutive modeling and numerical implementation. IBZ TU Dortmund, Germany, 3–7 September 2012. Available at: <http://www.lem3.fr/summerschool/00-Files/RD.pdf>.
- Desmorat R., On the Non Saturation of Cyclic Plasticity Law: A Power Law for Kinematic Hardening, in *Advanced Materials Modelling for Structures*, H. Altenbach and S. Kruch Eds., *Advanced Structured Materials* 19, 121–131.
- Desmorat R., 2015, Anisotropic damage modeling of concrete materials, *International Journal of Damage Mechanics*, 25(6), 818–852.
- Desmorat R., Mattiello A., Cormier J., 2017. A tensorial thermodynamic framework to account for the γ' rafting in nickel-based single crystal superalloys. *Int. J. Plast.* 95, 43–81.
- Diologent, F., Comportement en fluage et en traction de superalliages monocristallins à base de nickel. Thèse de doctorat, Université Paris XI Orsay, 2002. 5.
- Draper, S., Hull, D., Dreshfield, R., 1989. Observations of directional gamma prime coarsening during engine operation. *Met. Trans.* 20A , 683–688.
- Epishin, A. , Link, T., Portella, P., 2000. Bruckner, U., Evolution of the γ/γ' microstructure during high-temperature creep of a nickel-base superalloy. *Acta Mater.* 48, 4169–4177.
- Epishin, A., Link, T., Bruckner, U., Portella, P., 2001. Kinetics of the topological inversion of the γ/γ' microstructure during creep of a nickel-based superalloy. *Acta Mater.* 49, 4017–4023.
- Fedelich, B., Künecke, G., Epishin, A., Link, T., Portella, P., 2009. Constitutive modelling of creep degradation due to rafting in single crystals Ni-base superalloys. *Mat. Sci. Eng.* A510–511, 273–277.
- Fedelich, B., Epishin, A., Link, T., Klingelhöffer, H., Künecke G., Portella, P., 2012. Rafting during high temperature deformation in single crystal superalloy: experimental and modeling. E.S. Huron, R.C. Reed, M.C. Hardy, M.J. Mills, R. E. Montero, P.D. Portella, J. Telesman (Eds.) *Superalloys 2012*, TMS, Seven Springs, PA, USA, 491–500.
- Forté, S., Vianello, M., 1996. Symmetry classes for elasticity tensors 43 (2), 81–108.
- François, M., 1995. Identification des symétries matérielles de matériaux anisotropes. Ph.D. Thesis. Université Paris VI, Cachan (France).
- Gabrisch H., Kuttner T., Mukherji D., Chen W., Wahi R. P. and Wever H., 1994. Microstructural Evolution in the Superalloy SC16 Under Monotonic Loading. *Materials for Advanced Power Engineering*, Part II, 1119–1124.
- Gaffard V., Besson J., Gourgues-Lorenzon A.F., Creep failure model of a tempered martensitic stainless steel integrating multiple deformation and damage mechanisms, *Int. J. Fracture* 133 (2), 139–166, 2005.
- Ghighi J., Cormier J., Ostoja-Kuczynski E., Mendez J., Cailletaud G., Azzouz F., A microstructure sensitive approach for the prediction of the creep behaviour and life under complex loading paths. *Technische Mechanik*, 2012, 32, 205–220.
- Giraud R., 2013. Influence de l'histoire thermique sur les propriétés mécanique à haute et très haute température du superalliage monocristallin CMSX-4, Ph.D. Thesis, ENSMA-Université de Poitiers (France).
- Gorodentsev, A., *Algebra II: Textbook for Students of Mathematics*, Springer, 2017.
- le Graverend, J.B., Cormier, J., Gallerneau, F., Villechaise, P., Kruch, S., Mendez, J., 2014. A microstructure-sensitive constitutive modeling of the inelastic behavior of single crystal nickel-based superalloys at very high temperature. *Int. J. Plasticity* 59, 55–83.
- le Graverend J.B., Adrien J., Cormier J., 2017. Ex-situ X-ray Tomography Characterization of Porosity During High-Temperature Creep in a Ni-based Single-Crystal Superalloy: Toward Understanding What is Damage. *Mater. Sci. Eng. A* 695, 367–378.
- Gurson A.L., Continuum theory of ductile rupture by void nucleation and growth – part I. Yield criteria and flow rules for porous ductile media. *J. Eng. Mat. Tech.* 99, 2–15, 1977.
- Halphen, B., Nguyen, Q., 1975. Sur les matériaux standard généralisés. *J. de Mécanique* 14, 39–63.
- Hao S., Brocks W., The Gurson-Tvergaard-Needleman-model for rate and temperature-dependent materials with isotropic and kinematic hardening. *Computational Mechanics*, 20, 34–40, 1997.
- Hill, R.J., Rice, J.R., 1972. Constitutive Analysis of Elastic/Plastic Crystals at Arbitrary Strain. *J. Mec.Phy. Solids* 20, 401–413.
- Johnson G.R., Cook W.H., Fracture characteristics of three metals subjected to various strain, strain rates, temperatures and pressures, *Engng Fract. Mech.*, 2, pp. 31–48, 1985.
- Jun Chang H., Fivel M.C., Strudel J.-L., 2018, Micromechanics of primary creep in Ni base superalloys, *International Journal of Plasticity*, doi: 10.1016/j.ijplas.2018.04.009.
- Kachanov L. M., Time of the rupture process under creep conditions. *Izv. Akad. Nauk. SSR., (Otd. Tekh. Nauk.)*, 1958.
- Kamaraj M., 2003. Rafting in single crystal nickel-base superalloys: an overview. *Sadhana* 28, 115–128.
- Kaminski M., 2007, Modélisation de l'endommagement en fatigue des superalliages monocristallins pour aubes de turbines en zone de concentration de contrainte. PhD of Ecole Nationale Supérieure des Mines de Paris, in Mécanique.
- Kanatani, K., 1984. Distribution of directional data and fabric tensors. *Int. J. Eng. Sci.* 22, 14–164.
- Thomson (LordKelvin), W.K., 1856. Elements of a mathematical theory of elasticity. *Phil. Trans. R. Soc.* 166, 481.
- Thomson (LordKelvin), W.K., 1878. Elasticity, *Encyclopaedia Britannica*. Adam and Charles Black, Edinburgh.
- Kindrachuk V. and Fedelich V., 2012. Simulation of Non-Isothermal Mechanical Tests on a Single Crystal Nickel-Basis Super alloy. *Technische Mechanik* 32, 321–332.
- Krairi A., Doghri L., 2014. A thermodynamically-based constitutive model for thermoplastic polymers coupling viscoelasticity, viscoplasticity and ductile damage, *International Journal of Plasticity*, 60, 163–181.
- Leckie, F. and Onat, E. (1981). Tensorial Nature of Damage Measuring Internal Variables, In: Hult, J. and Lemaire, J. (eds), *Physical Non-linearities in Structural Analysis*, pp. 140–155, Springer, Berlin.
- Lemaitre J., Evaluation of dissipation and damage in metals, *Proceedings of I.C.M. Kyoto, Japan*, 1971.
- Lemaitre J., How to use damage mechanics, *Nuclear Engineering and Design*, 80(2), 233–245, 1984.
- Lemaitre, J., Chaboche, J. L., *Mécanique des matériaux solides*, Dunod 1985, *Mechanics of solid materials*, Oxford University Press, 1991 (english translation).
- Lemaitre, J., Chaboche, J. L., Benallal A., Desmorat R., *Mécanique des matériaux solides*, Dunod 3rd Edition 2009.
- Lemaitre, J., A course on damage mechanics, Springer Verlag, 1992.
- Lemaitre J., Desmorat R., *Engineering Damage Mechanics : Ductile, Creep, Fatigue and Brittle Failures*, Springer, 2005.
- Lemaitre J. and Dufailly J., Damage measurements, *Engineering Fracture Mechanics*, 28(5-6), 643–661, 1987.
- Lemaitre J., Doghri, Damage 90 : a post-processor for crack initiation, *Comput. Methods Appl. Mech. Eng.*, 115, pp. 197–232, 1994.
- Leblond J.-B., Perrin G., Suquet P., Exact results and approximate models for porous viscoplastic solids. *International Journal of Plasticity*, 10, 213–235, 1994.
- Lifshitz, I.M., Slyozov, V.V., 1961. *J. Phys. Chem. Solids* 19, 35–50.
- Ling C., Tanguy B., Besson J., Forest S., Latourte F., 2017. Void growth and coalescence in triaxial stress fields in irradiated FCC single crystals, *Journal of Nuclear Materials* 492, 157–170.
- Link T., Zabler S., Epishin A., Haibel A., Bansal M., Thibault X., 2006, *Materials Science and Engineering*, vol. A 425, 47–54, 2006.
- Lu L., Schwaiger R., Shan Z. W., Dao M., Lu K. and Suresh, S., 2005. Nano-sized twins induce high rate sensitivity of flow stress in pure copper, *Acta Mater.* 53(7) 2169–2179.
- Mahnken, R., 2002. Anisotropic creep modeling based on elastic projection operators with applications to CMSX-4 superalloy. *Comput. Method App. M.* 191, 1611–1637.
- MacKay, R.A., Ebert, L.J., 1985. The development of γ/γ' lamellar structures in a nickel-base superalloy during elevated temperature mechanical testing. *Met. Trans.* A 16A, 1969–1982.
- MacLachlan D. W., Gunturi G. S. K. and Knowles D. M., 2002. Modelling the uniaxial creep anisotropy of nickel base single crystal superalloys CMSX-4 and RR2000 at 1023 K using a slip system based finite element approach. *Computational Materials Science*, 25(1), 129–141.

- MacLachlan D. W. and Knowles D.M., 2001. The effect of material behaviour on the analysis of single crystal turbine blades. *Fatigue Fract. Engng. Mater. Struct.*, 25(November), 385-409.
- MacLachlan D.W., Wright L.W., Gunturi G.S.K., Knowles, D.M., 2001. Constitutive modeling of anisotropic creep deformation in single crystal blade alloys SRR99 and CMSX-4. *Int. J. Plasticity* 17, 441-467.
- Malcher L., Mamiya E.N., 2014. An improved damage evolution law based on continuum damage mechanics and its dependence on both stress triaxiality and the third invariant, *International Journal of Plasticity* 56, 232-261.
- Marull R., 2011. Plasticités cubiques et endommagement anisotrope induit pour les superalliages monocristallins sous chargement complexe, PhD of Ecole Normale Supérieure de Cachan, France.
- Marull R., Desmorat R., 2013, in *Advanced Materials Modelling for Structures*, H. Altenbach and S. Kruch Eds., *Advanced Structured Materials* 19, 2017-227.
- Matan N., Cox D., Rae C.M.F. and Reed R.C., 1999. On the kinetics of rafting in CMSX-4 superalloy single crystals, *Acta Mater.* 47, 2031-2045.
- Matan N., Cox D., Carter P., Rist M.A., Rae C., Reed R.C., 1999. Creep of CMSX-4 superalloy single crystals: effects of misorientation and temperature, *Acta Mater.* 47(15), 1549.
- Mbiakop A., Constantinescu A., Danas K., 2015. A model for porous single crystals with cylindrical voids of elliptical cross-section, *International Journal of Solids and Structures*, 64-65, pp.100-119.
- McLean M. and Dyson B.F., 2001. Modelling the effects of damage and microstructural evolution on the creep behaviour of engineering alloys. *Journal of engineering Materials and Technology* 122, 273-278.
- Mughrabi, H., 2009. Microstructural aspects of high temperature deformation of monocrystalline nickel base superalloys: some open problems. *Mater. Sci. Tech* 25, 191-204.
- Murakami S, Hayakawa K, Liu Y., 1998, Damage evolution and damage surface of elastic-plastic-damage materials under multiaxial loading, *Int. J. Damage Mech.*, 7, 103-28.
- Naumenko K., Altenbach H., Kutschke A., 2011, A Combined Model for Hardening, Softening, and Damage Processes in Advanced Heat Resistant Steels at Elevated Temperature, *Int. J. Damage Mech.*, 20, 578-597.
- Nouailhas, D., Cailletaud, G., 1995. Tension-torsion behavior of single crystal superalloys: experiment and finite element analysis. *Int. J. Plast.* 11, 451-470.
- Olive M., Kolev B., and Auffray N., A minimal integrity basis for the elasticity tensor, *Archive for Rational Mechanics and Analysis*, 1-31, 2017a.
- Olive M., Kolev B., Desmorat B., Desmorat R., Harmonic factorization and reconstruction of the elasticity tensor, *Journal of Elasticity*, 132, 67-101, 2017b.
- Onat, E. T., 1984. Effective properties of elastic materials that contain penny shaped voids. *Int. J. Eng. Sci.* 22, 1013-1021.
- Ostwald W., 1897. Studien über die Bildung und Umwandlung fester Körper, *Zeitschrift für physikalische Chemie* 22, 289-330.
- Orowan, E., 1948. Discussion on internal stress. In *Symposium on Internal Stresses in Metals*, 451-458.
- Pan J., Saje M., Needleman A., Localization of deformation in rate sensitive porous plastic solids, *Int. J. Fracture* 21, 261-278, 1983.
- Peirce, D., Asaro, R.J., Needleman A., 1983. Material rate dependence and localized deformation in crystalline solids. *Acta Metall.* 31, 1951-76.
- Pollock, T.M., Argon, A.S., 1994. Directional coarsening in nickel-base single crystals with high volume fractions of coherent precipitates, *Acta Metall. Mater.* 42, 1859-1874.
- Pollock T.M. and Tin S., 2006. Nickel-Based Superalloys for Advanced Turbine Engines: Chemistry, Microstructure, and Properties. *Journal of Propulsion and Power* 22(2), 361-374.
- Rabotnov Y. N., Creep problem in structural members, North Holland, Amsterdam, 1969.
- Reed, R.C., 2006. *The Superalloys - Fundamentals and Applications*, Cambridge University Press, Cambridge, UK.
- Reed, R.C., Matan, N., Cox, D.C., Rist, M.A., Rae, C.M.F., 1999. Creep of CMSX-4 superalloy single crystals: effects of rafting at high temperature, *Acta Mater.* 47, 3367-3381.
- Reed R. C., Cox D. C. and Rae C. M. F., 2007. Kinetics of rafting in a single crystal superalloy: effects of residual microsegregation. *Mater. Sci. Tech.* 23(8), 893-902.
- Rice, J.R., 1975. *Continuum Mechanics and Thermodynamics of Plasticity in Relation to Microscale Deformation Mechanisms. Constitutive Equations in Plasticity* (ed. A. S. Argon), M.I.T. Press, 23-79.
- Rice J.R., Tracey D.M., On the ductile enlargement of voids in triaxial stress fields, *J. Mech. Phys. Solids*, 17, 201-217, 1969.
- Roebuck B., Cox D. and R. Reed, 2001. The temperature dependence of γ' volume fraction in a Ni-based single crystal superalloy from resistivity measurements. *Scripta Mater.* 44 (6), 917-921
- Rychlewski J., 1984. On Hooke's Law, *Prikl. Matem. Mekhan.*, 48, 3, pp. 303-314.
- Saanouni K., Chaboche J.-L., Lesne P.M., On the creep crack-growth prediction by a non local damage formulation, *Eur. J. Mech. A/Solids*, 8, 437-459, 1989.
- Saanouni K., Forster C., Ben Hatira F., On the anelastic flow with damage, *International Journal of Damage Mechanics*, 3, 140-169, 1994.
- Schmid, E., Boas, W., 1935. *Kristallplastizität mit besonderer Berücksichtigung der Metalle*.
- Schouten J. A., *Tensor Analysis for Physicists*, Oxford, At the Clarendon Press, 1951.
- Sermage J.-P., *Fatigue thermique multiaxiale à température variable*, PhD thesis University Paris 6, France, 1998.
- Sermage J.P., Lemaitre J., Desmorat R., Multiaxial creep fatigue under anisothermal conditions, *Fatigue Fract. Engng. Mater. Struct.*, 23 (3), 241-252, 2000.
- Spencer A., A note on the decomposition of tensors into traceless symmetric tensors, *Int. J. Engng Sci.*, 8:475-481, 1970.
- Srivastava A. and Needleman A., 2015. Effect of crystal orientation on porosity evolution in a creeping single crystal, *Mechanics of Materials* 90, 10-29.
- Staroselsky, A., Cassenti, B., 2008, Mechanisms for tertiary creep of single crystal superalloy, *Mech. Time-Depend. Mater.* 12, 275-289.
- Staroselsky, A., Cassenti, B.N., 2011. Creep, plasticity and fatigue on single crystal superalloys, *Inter. J. of Sol. & Struc.* 48, 2060-2075.
- Steuer S., Villechaise P., Pollock T.M. and Cormier J., 2015. Benefits of high gradient solidification for creep and low cycle fatigue of AM1 single crystal superalloy, *Material Science and Engineering A* (645), 109-115.
- Steckmeyer A., Caractérisation et modélisation du comportement mécanique à haute température des aciers ferritiques renforcés par dispersion d'oxydes. PhD of Ecole Nationale Supérieure des Mines de Paris, 2012.
- Svoboda J., Lukas P., 1998. Model of creep in (001)-oriented superalloys single crystals. *Acta Mater.* 46, 3421-3431.
- Tinga, T., Brekelmans, W.A.M., Geers, M.G.D., 2009. Directional coarsening in nickel-base superalloys and its effect on the mechanical properties. *Computational Mater. Sci.* 47, 471-481.
- Tinga, T., Brekelmans, W.A.M., Geers, M.G.D., 2009, Time-incremental creep-fatigue damage rule for single crystal Ni-base superalloys, *Materials Science and Engineering A* 508, 200-228.
- Tien, J. K., and Copley, S., M., 1971. The effect of orientation and sense of applied uniaxial stress on the morphology of coherent gamma prime precipitates in stress annealed nickel-base superalloy crystals, *Met. Trans.* 2, 543-553.
- Tien, J. K., Gamble, R. P., 1971. Effects of stress coarsening on coherent particle strengthening. *Met. Trans.* 3, 2157-2162.
- Tinga, T., Brekelmans, W.A.M., Geers, M.G.D., 2009. Directional coarsening in nickel-base superalloys and its effect on the mechanical properties. *Computational Mater. Sci.* 47, 471-481.
- Thebaud L., Villechaise P., Cormier J., Hamon F., Crozet C., Devaux A., Francher A., Rouffié A.L., Organista A., Relationships between microstructural parameters and time dependent properties of a new Ni based superalloy AD730™, *Superalloys 2016: Proceedings of the 13th International Symposium on Superalloys* Edited by: Mark Hardy, Eric Huron, Uwe Glatzel, Brian Griffin, Beth Lewis, Cathie Rae,

- Venkat Seetharaman, and Sammy Tin TMS (The Minerals, Metals & Materials Society), 877-886, 2016.
- Tvergaard V., Needleman A., Analysis of the cup-cone fracture in a round tensile bar, *Acta Metall.* 32, 157–169, 1984.
- Tvergaard V. and Needleman A., Effect of material rate sensitivity on failure modes in the Charpy V-notch test, *J. Mech. Phys. Solids*, 34 (3), 213–241, 1986.
- von Mises R., *Mechanics der plastischen Formänderung von Kristallen*, *Zeitschrift Angewandte Mathematik Mechanik (ZAMM)*, 8, 161–185, 1928.
- Wagner C. , 1961. Theorie der alterung von niederschlägen durch umlösen. *Zeitschrift für Elektrochemie*, 65, 581–591.
- Zhang W.J., 2016. Thermal mechanical fatigue of single crystal superalloys: Achievements and challenges. *Materials Science and Engineering A* (650), 389-395.